

JAERI-Data/Code
95-004



PKN-H:
A POINT KERNEL SHIELDING CODE FOR NEUTRON SOURCE
UP TO 400 MeV

June 1995

Hiroshi KOTEGAWA, Yukio SAKAMOTO
and Shun-ichi TANAKA

日本原子力研究所
Japan Atomic Energy Research Institute

本レポートは、日本原子力研究所が不定期に公刊している研究報告書です。

入手の問合せは、日本原子力研究所技術情報部情報資料課（〒319-11 茨城県那珂郡東海村）あて、お申し越しください。なお、このほかに財団法人原子力弘済会資料センター（〒319-11 茨城県那珂郡東海村日本原子力研究所内）で複写による実費頒布をおこなっております。

This report is issued irregularly.

Inquiries about availability of the reports should be addressed to Information Division, Department of Technical Information, Japan Atomic Energy Research Institute, Tokaimura, Naka-gun, Ibaraki-ken 319-11, Japan.

© Japan Atomic Energy Research Institute, 1995

編集兼発行 日本原子力研究所
印 刷 いばらき印刷株

PKN-H : A Point Kernel Shielding Code
for Neutron Source Up to 400 MeV

Hiroshi KOTEGAWA, Yukio SAKAMOTO and Shun-ichi TANAKA

Department of Reactor Engineering
Tokai Research Establishment
Japan Atomic Energy Research Institute
Tokai-mura, Naka-gun, Ibaraki-ken

(Received April 3, 1995)

A point-kernel integral technique code PKN-H, and the related data library have been developed to calculate neutron and secondary gamma-ray dose equivalents in water, ordinary concrete and iron shields for neutron source up to 400MeV in 3-dimensional geometry. The comparison between calculational results of the present code and the those of sophisticated transport calculation codes, such as 1-dimensional transport code ANISN-JR, the 2-dimensional transport code DOT and continuous energy Monte Carlo code MCNP, showed a sufficient agreement for practical purpose, and the availability of the PKN-H code has been verified.

Keywords: Point Isotropic Source, Neutron, Secondary Gamma-ray, Dose Equivalent, Water, Concrete, Iron, Point Kernel Technique, PKN-H, HILO86R, Infinite Medium Effect

PKN-H : 400MeVまでの中性子線源に対する点滅衰核遮蔽計算コード

日本原子力研究所東海研究所原子炉工学部
小手川 洋・坂本 幸夫・田中 俊一

(1995年4月3日受理)

3次元的に分布した400MeVまでの中性子線源に対して、水、普通コンクリートと鉄の遮蔽体を透過した中性子と2次 γ 線の線量当量を計算できる点滅衰核積分計算コードPKN-H及びその為のデータライブラリーを作成した。典型的な遮蔽体系についてのPKN-Hコードの計算結果を、1次元輸送計算コードANISN-JR、2次元輸送計算コードDOT4.2、及び3次元連続エネルギーモンテカルロ輸送計算コードMCNPの計算結果と比較したところ、計算精度について実用上良い結果が得られ、コードの有用性が確認された。

Contents

1. Introduction	1
2. Analytical Formulation of Point-kernel Code PKN-H	1
2.1 Single-layer Shield	1
2.2 Point Kernel for Single-layer Shield	3
2.3 Multilayer Shields	3
2.4 Correction for Infinite Medium	5
3. Sample Calculations and Comparisons of the Results	6
4. Summary	9
References	9
Appendix	30

目 次

1. 序	1
2. 点減衰核積分法 PKN-H の解析式	1
2.1 単層遮蔽	1
2.2 単層に対する点減衰核	3
2.3 多重層遮蔽	3
2.4 無限媒質補正	5
3. 計算例と結果の比較	6
4. まとめ	9
参考文献	9
付 錄	30

1. Introduction

Recently, the present authors have produced the attenuation data of neutron and secondary gamma-ray dose equivalents for point isotropic neutron sources up to 400 MeV in water, ordinary concrete and iron¹, with ANISN-JR², code and HIL086R cross section data³, and represented the attenuation data with a polynomial function.

In the present work, a point kernel integral technique code PKN-H is developed for shielding calculations of high energy neutrons based on the previous work. In the PKN-H code the data base of neutron and secondary gamma-ray dose equivalents in infinite shields of water, ordinary concrete and iron for point isotropic neutron sources of 0.01 MeV to 400 MeV are included, and also the data to correct the excess overestimation for finite shields originated from the attenuation data in infinite shields. Moreover, the combinatorial geometry(CG) technique is used in the code to represent the source and shield geometries of 3 dimensional configuration. In this report, the basic formula used in the PKN-H code is presented to calculate the dose equivalents, and the performance is discussed by comparing the results of the PKN-H with those of ANISN-JR, DOT4.2⁴, and MCNP⁵, for typical shielding problems. Besides, the input and output samples for the shielding problems are demonstrated with the input data instruction. Geometrical routine of PKN-H program are mainly based on that of QAD-P5A program⁶, and, especially, CG routine installed in PKN-H owe to MORSE-CG program⁷.

2. Analytical Formulation of Point-Kernel Code PKN-H

2.1 Single-Layer Shield

In point kernel technique method, the neutron or secondary gamma-ray dose equivalent rate $H(r_R)$ at a coordinate r_R in spherical geometry is represented, as follows,

$$H(r_R) = \int dE \int dr S(E, r) \times h(E, r, r_R) \times \frac{1}{4\pi |r - r_R|^2}, \quad (2.1)$$

1. Introduction

Recently, the present authors have produced the attenuation data of neutron and secondary gamma-ray dose equivalents for point isotropic neutron sources up to 400 MeV in water, ordinary concrete and iron¹, with ANISN-JR², code and HIL086R cross section data³, and represented the attenuation data with a polynomial function.

In the present work, a point kernel integral technique code PKN-H is developed for shielding calculations of high energy neutrons based on the previous work. In the PKN-H code the data base of neutron and secondary gamma-ray dose equivalents in infinite shields of water, ordinary concrete and iron for point isotropic neutron sources of 0.01 MeV to 400 MeV are included, and also the data to correct the excess overestimation for finite shields originated from the attenuation data in infinite shields. Moreover, the combinatorial geometry(CG) technique is used in the code to represent the source and shield geometries of 3 dimensional configuration. In this report, the basic formula used in the PKN-H code is presented to calculate the dose equivalents, and the performance is discussed by comparing the results of the PKN-H with those of ANISN-JR, DOT4.2⁴, and MCNP⁵, for typical shielding problems. Besides, the input and output samples for the shielding problems are demonstrated with the input data instruction. Geometrical routine of PKN-H program are mainly based on that of QAD-P5A program⁶, and, especially, CG routine installed in PKN-H owe to MORSE-CG program⁷.

2. Analytical Formulation of Point-Kernel Code PKN-H

2.1 Single-Layer Shield

In point kernel technique method, the neutron or secondary gamma-ray dose equivalent rate $H(r_R)$ at a coordinate r_R in spherical geometry is represented, as follows,

$$H(r_R) = \int dE \int dr S(E, r) \times h(E, r, r_R) \times \frac{1}{4\pi |r - r_R|^2}, \quad (2.1)$$

where S and h mean source spectrum and attenuation kernel, respectively. Double integral runs over source energy and full volume of source. The integral form is rewritten as

$$= \sum_j \sum_i S_{j,i} \times h_j(r_i, r_R) \times \frac{1}{4\pi |r_i - r_R|^2}, \quad (2.2)$$

where

- i : index about source coordinates,
- j : index about source energy,
- $S_{j,i}$: source intensity for source coordinate i and source energy j ,
- r_i : coordinate of source.

Attenuation kernel $h_j(r_i, r_R)$ expresses the attenuation of dose equivalent except geometrical attenuation $1 / 4\pi |r_i - r_R|^2$, which depends on source neutron energy E (correspond to energy index j) and coordinates of source location r_i .

Source $S_{j,i}$ is assumed to be represented by a product of energy dependent part s_j and spacial dependent part s_i .

$$H(r_R) = \sum_j s_j \times \sum_i s_i \times h_j(r_i, r_R) \times \frac{1}{4\pi |r_i - r_R|^2}. \quad (2.3)$$

Moreover, the point kernel $h_j(r_i, r_R)$ is approximated by a polynomial exponent function with respect to the distance $|r_i - r_R|$, as follows,

$$h_j(r_i, r_R) = \exp(G_j(r_i, r_R)), \quad (2.4)$$

$$G_j(r_i, r_R) = \sum_{m=1}^N a_{mj}^{N_m} x r^{m-1} x \theta_+(r) + (b_j x r + g(r)) x \theta_-(r), \quad (2.5)$$

where $r = |r_i - r_R|$,

$$\theta_+(r) = \frac{1}{2|r_e-r|} \cdot \frac{\{|r_e-r| - (r_e-r)\}}{(r_e-r)} \quad (2.6)$$

$$\theta_-(r) = 1 - \theta_+(r_e-r), \quad (2.7)$$

$$g(r) = \ln(4\pi r^2) \quad \text{for water and concrete} \quad (2.8)$$

$$= 0 \quad \text{for iron} \quad (2.9)$$

and $a_{m,j}^N$: m-th parameter in the system consists N parameters for source energy j,
 r_e : conjunction radius,
 b_j : effective attenuation parameter at far distance from source.

2.2 Point Kernel for Single-Layer Shield

The dose equivalents for single-layer shield are calculated using Eq.(2.3). In this context, the point kernel data which is determined by the attenuation factors in shields is the most essential one for PKN-H code. In Tables 2.1 and 2.2 are summarized the calculational conditions and material composition for the calculations of the attenuation factors. In the PKN-H code, the attenuation data for monoenergetic neutrons of 52 energy group shown in Table 2.3 are represented by polynomial functions of which the parameters have been obtained in the previous work¹. Besides, the data for ²⁵²Cf fission and ²⁴¹Am-Be neutron sources are also contained for convenience, because the shielding calculations for these sources are often required.

2.3 Multilayer Shields

In the PKN-H code, dose equivalents in multi-layer shields are calculated by applying the point kernel for single layer.

Figure 2.1 shows an example of multi-layer shields, where a point isotropic monoenergetic neutron source is placed in shields of M1 having radius r_1 and M2 having thickness r_2-r_1 . In this case, the

neutron dose equivalent up to r_1 is the same as that of single-layer for the shield M1, while the dose equivalent for the thickness of $r_1 \leq r \leq r_2$ in the shield M2 is calculated as follows:

1) The first layer is replaced by an equivalent thick shield of second layer material so as the attenuation is equal. When the dose equivalent at r_1 of the first layer is equal to that of a thickness r_{EQ} of the second layer, the first layer in Fig.2.1 is replaced by the second layer material having a thickness r_{EQ} . That is, the relation is given by

$$H_n(r_{EQ}, 1)_{M2} = H_n(r_1)_{M1}, \quad (2.10)$$

where $H_n(r_1)_{M1}$ and $H_n(r_{EQ}, 1)_{M2}$ are the neutron dose equivalents at the thickness of r_1 in M1 and r_{EQ} in M2, respectively.

2) The dose equivalent for $r_1 \leq r \leq r_2$ is given by a corresponding one to the second layer shield with a thickness of $r_{EQ} + (r - r_1)$.

3) When there are n-fold multilayer between neutron source and detector point, neutron dose equivalent at a detector point of $r_{n-1} \leq r \leq r_n$ in a shield material M_n of n-th layer shield from source is obtained by repeating the similar procedure, and the equivalent thickness $r_{EQ,n-1}$ up to n-th layer is obtained based on the following equation,

$$H_n(r_{EQ,n-1})_{M_n} = H_n(r_{EQ,n-2} - r_{n-2} + r_{n-1})_{M_{n-1}}. \quad (2.11)$$

The secondary gamma-ray dose equivalent for multilayer is also calculated by the same procedure with that for neutrons.

In Figs.2.2 to 2.13, the dose equivalents by the present procedure are compared with those with the ANISN-JR code concerning the double layer composed of water, ordinary concrete and iron for 50 MeV and 100 MeV neutrons. As seen in Fig.2.2 and 2.3, the present procedure is applied successfully for the arrangement of the first layer of water and the second one of ordinary concrete, although the results of PKN-H are a little bit smaller than those of ANISN-JR. For the opposite arrangement, the PKN-H calculations overestimate the ANISN-JR calculations as shown in Figs.2.4 and 2.5. As to the combinations of ordinary concrete and iron or water and iron, as seen in Figs. 2.6 to 2.13, the PKN-H calculations overestimate largely the

ANISN-JR ones when ordinary concrete or water are arranged as the second-layer shield, while the neutron dose equivalent with the PKN-H becomes a little smaller when iron is used as the second layer. Consequently, we are able to summarize these features as

- 1) when a shield containing more hydrogen is used as the first layer, the neutron dose with the PKN-H becomes a little underestimation, while the estimation of second gamma-ray dose is almost reasonable except for 400 MeV neutron source.
- 2) when more hydrogenous shield is arranged for the second layer, the PKN-H calculations overestimate largely.

The neutron spectrum is changed very much in the vicinity of the boundary of the two layers, and especially thermal neutrons are built up in water and ordinary concrete, and after that it is absorbed strongly in iron to produce secondary gamma-rays. The present procedure employed in the PKN-H code is unable to follow these behavior. Therefore more discreet consideration should be done for the justification of the results of multi-layer with the PKN-H code.

2.4 Correction for Infinite Medium

In general, radiation shields are composed of materials of finite thickness, while the present attenuation factors are calculated for infinite thickness shields. Therefore, the dose equivalents calculated using the present data would overestimate those for real shields by albedo component. It has been demonstrated that the overestimation exceed a few factors in some cases.¹³ Thus, the infinite medium effect data which has been obtained in the previous work¹³ was installed to correct the infinite medium effect in PKN-H code.

Using the data of the infinite medium effect, the neutron and secondary gamma-ray dose equivalents for a finite shield of thickness r ; $H_n^*(r)_{mn}$ and $H_\gamma^*(r)_{mn}$, are estimated by the following equations,

$$H_n^*(r)_{mn} =$$

$$\sum_j C_{nj}(r_{EQ,n-1})_{mn-1} \times s_j \times H_{nj}(r_{EQ,n-1}-r_{n-1}+r)_{mn}, \quad (2.12)$$

$$H_\gamma^*(r)_{mn} =$$

$$\Sigma_j C_{\gamma,j}(r_{EQ,n-1})_{Mn-1} \times S_j \times H_{\gamma,j}(r_{EQ,n-1}-r_{n-1}+r)_{Mn}, \quad (2.13)$$

where $C_{n,j}(r_{EQ,n-1})_{Mn-1}$ and $C_{\gamma,j}(r_{EQ,n-1})_{Mn-1}$ are the infinite medium effect for neutrons and secondary gamma-ray dose equivalents. In case of multilayer shields, the values for n-th layer are obtained as those at $r_{EQ,n-1}+(r_n-r_{n-1})$.

3. Sample Calculations and Comparisons of the Results

Five kinds of sample calculations were made with the PKN-H code, and compared with those of ANISN-JR, DOT4.2, MCNP-4A and QAD-P5A⁶⁾ codes to verify the availability. The input manual for PKN-H code is given in Appendix A.1, and the input sample data for the sample calculations and the calculated results are represented in Appendices A.2 to A.6 and A.8 to A.12, respectively.

Sample 1 : Dose equivalent calculation for a ^{252}Cf point source placed at the center of polyethylene spherical shell of 5 cm thickness having an inner radius of 30 cm.
 (See Fig.3.1).

Polyethylene is substituted by water, because no data is prepared for polyethylene. The input data of sample problem-1 is given in Appendix A.2.

Both of neutron and secondary gamma-ray dose equivalents for infinite thickness and for finite one corrected with the infinite effect are calculated with the PKN-H code shown in Appendix A.8. The both values are compared with those of ANISN-JR and MCNP in Fig.3.2. The results with PKN-H are in good agreement with those of ANISN-JR and MCNP up to 35 cm. The doses in infinite thickness represented by PKN-H/inf, however, show overestimation because of the infinite effect. On the contrary, the values denoted by PKN-H/fini for which the infinite effect has been corrected are in reasonable agreement.

$$\Sigma_j C_{\gamma,j}(r_{EQ,n-1})_{Mn-1} \times S_j \times H_{\gamma,j}(r_{EQ,n-1}-r_{n-1}+r)_{Mn}, \quad (2.13)$$

where $C_{n,j}(r_{EQ,n-1})_{Mn-1}$ and $C_{\gamma,j}(r_{EQ,n-1})_{Mn-1}$ are the infinite medium effect for neutrons and secondary gamma-ray dose equivalents. In case of multilayer shields, the values for n-th layer are obtained as those at $r_{EQ,n-1}+(r_n-r_{n-1})$.

3. Sample Calculations and Comparisons of the Results

Five kinds of sample calculations were made with the PKN-H code, and compared with those of ANISN-JR, DOT4.2, MCNP-4A and QAD-P5A⁶⁾ codes to verify the availability. The input manual for PKN-H code is given in Appendix A.1, and the input sample data for the sample calculations and the calculated results are represented in Appendices A.2 to A.6 and A.8 to A.12, respectively.

Sample 1 : Dose equivalent calculation for a ^{252}Cf point source placed at the center of polyethylene spherical shell of 5 cm thickness having an inner radius of 30 cm.
 (See Fig.3.1).

Polyethylene is substituted by water, because no data is prepared for polyethylene. The input data of sample problem-1 is given in Appendix A.2.

Both of neutron and secondary gamma-ray dose equivalents for infinite thickness and for finite one corrected with the infinite effect are calculated with the PKN-H code shown in Appendix A.8. The both values are compared with those of ANISN-JR and MCNP in Fig.3.2. The results with PKN-H are in good agreement with those of ANISN-JR and MCNP up to 35 cm. The doses in infinite thickness represented by PKN-H/inf, however, show overestimation because of the infinite effect. On the contrary, the values denoted by PKN-H/fini for which the infinite effect has been corrected are in reasonable agreement.

Sample 2 : Dose equivalent calculation for a ^{252}Cf volume source along A-line, B-line, and C-line in water as shown in Fig.3.3, where the ^{252}Cf neutron source is uniformly distributed in cylinder of 25 cm radius and 50 cm height of water.

The input data of sample problem-2 is given in Appendix A.3 and output data is given in Appendix A.9. In Figs. 3.4 and 3.5, the calculated results are shown with those by ANISN-JR and DOT4.2 codes, where the abscissa is the distance from center axis of the cylinder.

For neutrons shown in Fig.3.4, the PKN-H calculations along the A-line agree well with those of ANISN-JR code except for a little discrepancy around the source region due to the geometrical steep attenuation near the source region. On the other hand, the PKN-H calculations are fairly larger than those of the DOT4.2, and increases with the distance. This may be attributed to the insufficient angular quadratures of the DOT4.2 code. As for secondary gamma-rays as seen in Fig.3.5, the values of PKN-H shows relatively a good agreement with the DOT4.2, since the secondary gamma-ray source is distributed and the effect of angular quadrature becomes smaller.

Sample 3 : Dose equivalent calculation for distributed ^{252}Cf sources in a cylindrical polyethylene container (25cm radius and 57.5cm height). Four ^{252}Cf iod sources of 2cm radius and 15cm height are contained in the container as shown in Fig.3.6.

The input data of sample problem-3 is given in Appendix A.4 and output data is given in Appendix A.10. Polyethylene is substituted by water, because no data is prepared for polyethylene.

Figure 3.7 shows neutron and Fig.3.8 secondary gamma-ray dose equivalents calculated with the PKN-H and ANISN-JR codes. Neutron and secondary gamma-ray dose equivalents, as seen in PKN-H/inf of Figs.3.7 and 3.8, the results with the PKN-H without infinite medium effect correction overestimates in some extent at boundary between polyethylene and air in comparison with that of ANISN-JR, while PKN-

H/fini's in Figs.3.7 and 3.8, which are corrected with the infinite effect, show a better agreement with that of ANISN-JR.

Sample 4 : Dose equivalent calculation for a ^{252}Cf source in a room of concrete of 40 cm thickness. The ^{252}Cf of 2 cm radius and 15 cm height contained a cylindrical polyethylene which is set at a corner of the room as shown in Figs.3.9(1) and 3.9(2).

This sample is an example of multilayer shield, in which a procedure mentioned in Sec. 2.3 is carried out in the PKN-H code. Calculations have been performed at the hight of source center along y-direction, and z-direction in Fig.3.9(2), where the polyethylene is replaced by water. The input data of sample problem-4 is given in Appendix A.5 and output data is given in Appendix A.11. Calculational results for y- direction are shown in Figs.3.10 and 3.11.

The results between the PKN-H and other codes are in good agreement, although the DOT4.2 calculation is smaller than others. Figure 3.12 shows the results with PKN-H code along the z-direction from the floor to the ceiling. Good agreement is observed between the results of PKN-H and ANISN-JR concerning both neutron and secondary gamma-ray dose equivalents.

Sample 5 : Lateral dose equivalent calculation through ordinary concrete tunnel for 250 MeV point neutron source at the center axis. The neutron source is located at the center of axis of 9 m thick cylindrical tunnel of which inner radius is 1 m. (See Fig.3.13)

The input data of sample problem-5 is given in Appendix A.6 and the output result is given in Appendix A.12. Figures 3.14 and 3.15 show calculational results of neutron and secondary gamma-ray dose equivalent, respectively.

For both neutron and secondary gamma-ray dose equivalents, the results of the PKN-H calculation agree well with those of ANISN-JR from inner surface of concrete to 10 m in radius.

The PKN-H/inf shows a little overestimation outside the concrete, but if the correction of the infinite effect is taken into account, better agreement is obtained as shown by the PKN-H/fini.

4. Summary

A point-kernel integral calculation code PKN-H, by which the neutron and secondary gamma-ray dose equivalents are calculated for monoenergetic neutron volume source up to 400 MeV in 3-dimensional geometry, has been developed. The availability of the PKN-H code has been verified by comparing with other sophisticated transport codes; ANISN-JR, DOT4.2 and MCNP-4A.

References

- 1) Kotegawa,H. et al.: "Attenuation data of point isotropic neutron sources up to 400MeV in the shielding materials of water, concrete and iron", JAERI-Data/Code 94-003(1994).
- 2) Engle,W.W.,Jr.: "ANISN:A One-Dimensional Discrete Ordinates Transport Code", CCC-82(1967).
Koyama,K. et.al:"ANISN-JR:A One-Dimensional Discrete Ordinates Code for Neutron and Gamma-Ray Transport Calculation",JAERI-M 6954(1977)., Koyama,K. et.al:"Multi-Group Cross Section Sets for Shield Materials -100 Neutron Group and 20 Gamma-Ray Groups in P_5 Approximation-",JAERI-M 6928(1977).
- 3) Kotegawa,H. and Tanaka,S.: "Neutron-photon multigroup cross sections for neutron energies up to 400MeV:HIL086R -Revision of HIL086 Library-",JAERI-M 93-020(1993).
- 4) Rhoades,W.A.; "DOT-IV:Two Dimensional Discrete Ordinates Transport Code System", CCC-320(1970).
- 5) ORNL-RSIC Computer Code Collection,CCC-200/MCNP-4A.
- 6) Solomito,E. and Stockton,J.: "Modification of the point-kernel code QAD-P5A:Conversion to the IBM-360 computer and incorporation of additional geometry routines",ORNL-H-181(1968).
- 7) ORNL-RSIC Computer Code Collection,CCC-203/MORSE-CG.

The PKN-H/inf shows a little overestimation outside the concrete, but if the correction of the infinite effect is taken into account, better agreement is obtained as shown by the PKN-H/fini.

4. Summary

A point-kernel integral calculation code PKN-H, by which the neutron and secondary gamma-ray dose equivalents are calculated for monoenergetic neutron volume source up to 400 MeV in 3-dimensional geometry, has been developed. The availability of the PKN-H code has been verified by comparing with other sophisticated transport codes; ANISN-JR, DOT4.2 and MCNP-4A.

References

- 1) Kotegawa,H. et al.: "Attenuation data of point isotropic neutron sources up to 400MeV in the shielding materials of water, concrete and iron", JAERI-Data/Code 94-003(1994).
- 2) Engle,W.W.,Jr.: "ANISN:A One-Dimensional Discrete Ordinates Transport Code", CCC-82(1967).
Koyama,K. et.al:"ANISN-JR:A One-Dimensional Discrete Ordinates Code for Neutron and Gamma-Ray Transport Calculation",JAERI-M 6954(1977)., Koyama,K. et.al:"Multi-Group Cross Section Sets for Shield Materials -100 Neutron Group and 20 Gamma-Ray Groups in P_5 Approximation-",JAERI-M 6928(1977).
- 3) Kotegawa,H. and Tanaka,S.: "Neutron-photon multigroup cross sections for neutron energies up to 400MeV:HIL086R -Revision of HIL086 Library-",JAERI-M 93-020(1993).
- 4) Rhoades,W.A.; "DOT-IV:Two Dimensional Discrete Ordinates Transport Code System", CCC-320(1970).
- 5) ORNL-RSIC Computer Code Collection,CCC-200/MCNP-4A.
- 6) Solomito,E. and Stockton,J.: "Modification of the point-kernel code QAD-P5A:Conversion to the IBM-360 computer and incorporation of additional geometry routines",ORNL-H-181(1968).
- 7) ORNL-RSIC Computer Code Collection,CCC-203/MORSE-CG.

The PKN-H/inf shows a little overestimation outside the concrete, but if the correction of the infinite effect is taken into account, better agreement is obtained as shown by the PKN-H/fini.

4. Summary

A point-kernel integral calculation code PKN-H, by which the neutron and secondary gamma-ray dose equivalents are calculated for monoenergetic neutron volume source up to 400 MeV in 3-dimensional geometry, has been developed. The availability of the PKN-H code has been verified by comparing with other sophisticated transport codes; ANISN-JR, DOT4.2 and MCNP-4A.

References

- 1) Kotegawa,H. et al.: "Attenuation data of point isotropic neutron sources up to 400MeV in the shielding materials of water, concrete and iron", JAERI-Data/Code 94-003(1994).
- 2) Engle,W.W.,Jr.: "ANISN:A One-Dimensional Discrete Ordinates Transport Code", CCC-82(1967).
Koyama,K. et.al:"ANISN-JR:A One-Dimensional Discrete Ordinates Code for Neutron and Gamma-Ray Transport Calculation",JAERI-M 6954(1977)., Koyama,K. et.al:"Multi-Group Cross Section Sets for Shield Materials -100 Neutron Group and 20 Gamma-Ray Groups in P_5 Approximation-",JAERI-M 6928(1977).
- 3) Kotegawa,H. and Tanaka,S.: "Neutron-photon multigroup cross sections for neutron energies up to 400MeV:HIL086R -Revision of HIL086 Library-",JAERI-M 93-020(1993).
- 4) Rhoades,W.A.; "DOT-IV:Two Dimensional Discrete Ordinates Transport Code System", CCC-320(1970).
- 5) ORNL-RSIC Computer Code Collection,CCC-200/MCNP-4A.
- 6) Solomito,E. and Stockton,J.: "Modification of the point-kernel code QAD-P5A:Conversion to the IBM-360 computer and incorporation of additional geometry routines",ORNL-H-181(1968).
- 7) ORNL-RSIC Computer Code Collection,CCC-203/MORSE-CG.

Table 2.1 Calculational conditions of ANISN-JR for attenuation parameters installed in PKN-H code.

Code	ANISN-JR ^{**} : 1-dimensional discrete ordinates transport calculation code		
Cross section library	HIL086R ^{**} : (P_5) effective macroscopic cross section		
Number of energy groups	neutron 66 groups gamma-ray 22 groups		
Source	Point isotropic : 55 monoenergetic neutrons (from 0.01MeV to 400MeV), ^{252}Cf fission and $^{241}\text{Am-Be}$ neutrons		
Shielding materials	water, ordinary concrete and iron		
Geometry	1-dimensional sphere (S_{16})		
Flux to dose equivalent conversion factor	neutron	$E > 20$ MeV	maximum dose equiv. ^{**}
		$E < 20$ MeV	1cm depth dose equiv. ^{***}
	gamma-ray	$E > 10$ MeV	maximum dose equiv. ^{**}
		$E < 10$ MeV	1cm depth dose equiv. ^{***}

*) ICRP Publication 51(1987), p.39, Table 23.

**) ibid., p.36, Table 21.

+) ibid., p.26, Table 14.

++) ibid., p.22, Table 10.

Table 2.2 Atomic number densities.

unit($10^{24}/\text{cm}^3$)

	Water	Ordinary concrete***	Iron
H	6.6738×10^{-2} *	1.3851-2	
C		1.1542-4	
N			
O	3.3369-2	4.5921-2	
Mg		1.2388-4	
Al		1.7409-3	
Si		1.6621-2	
K		4.6205-4	
Ca		1.5025-3	
Fe		3.4510-4	8.4869-2
density (g/cm^3)	1.00	2.27	7.87

*) JAERI-M 6928(1977).

**) Type 02-a concrete, ANL-5800, p.660(1963).

+) read as 6.6738×10^{-2}

Table 2.3 Group numbers and energy group structure of source neutrons
in units of MeV.

Group	Energy Range	Group	Energy Range
-1	$^{241}\text{Am-Be}$	27	2.750E+01 - 2.500E+01
0	^{252}Cf	28	2.500E+01 - 2.250E+01
		29	2.250E+01 - 1.960E+01
		30	1.960E+01 - 1.750E+01
1	4.000E+02 - 3.750E+02	31	1.750E+01 - 1.490E+01
2	3.750E+02 - 3.500E+02	32	1.490E+01 - 1.350E+01
3	3.500E+02 - 3.250E+02	33	1.350E+01 - 1.220E+01
4	3.250E+02 - 3.000E+02	34	1.220E+01 - 1.000E+01
5	3.000E+02 - 2.750E+02	35	1.000E+01 - 8.190E+00
6	2.750E+02 - 2.500E+02	36	8.190E+00 - 6.700E+00
7	2.500E+02 - 2.250E+02	37	6.700E+00 - 5.490E+00
8	2.250E+02 - 2.000E+02	38	5.490E+00 - 4.490E+00
9	2.000E+02 - 1.800E+02	39	4.490E+00 - 3.680E+00
10	1.800E+02 - 1.600E+02	40	3.680E+00 - 3.010E+00
11	1.600E+02 - 1.400E+02	41	3.010E+00 - 2.460E-00
12	1.400E+02 - 1.200E+02	42	2.460E+00 - 2.020E-00
13	1.200E+02 - 1.100E+02	43	2.020E+00 - 1.650E-00
14	1.100E+02 - 1.000E+02	44	1.650E+00 - 1.350E-00
15	1.000E+02 - 9.000E+01	45	1.350E+00 - 1.110E-00
16	9.000E+01 - 8.000E+01	46	1.110E+00 - 9.070E-01
17	8.000E+01 - 7.000E+01	47	9.070E-01 - 7.430E-01
18	7.000E+01 - 6.500E+01	48	7.430E-01 - 4.980E-01
19	6.500E+01 - 6.000E+01	49	4.980E-01 - 3.340E-01
20	6.000E+01 - 5.500E+01	50	3.340E-01 - 2.240E-01
21	5.500E+01 - 5.000E+01	51	2.240E-01 - 1.500E-01
22	5.000E+01 - 4.500E+01	52	1.500E-01 - 8.650E-02
23	4.500E+01 - 4.000E+01	53	8.650E-02 - 3.180E-02
24	4.000E+01 - 3.500E+01	54	3.180E-02 - 1.500E-02
25	3.500E+01 - 3.000E+01	55	1.500E-02 - 7.100E-03
26	3.000E+01 - 2.750E+01		

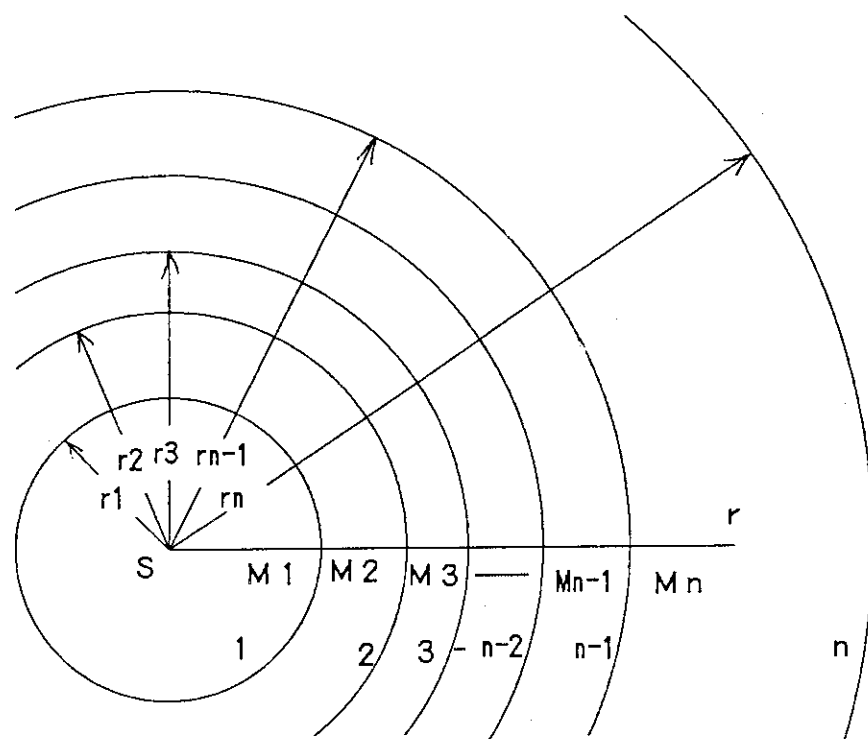


Fig. 2.1 The definition of equivalent length for neutron and secondary gamma ray dose equivalent calculation in multi-layer.

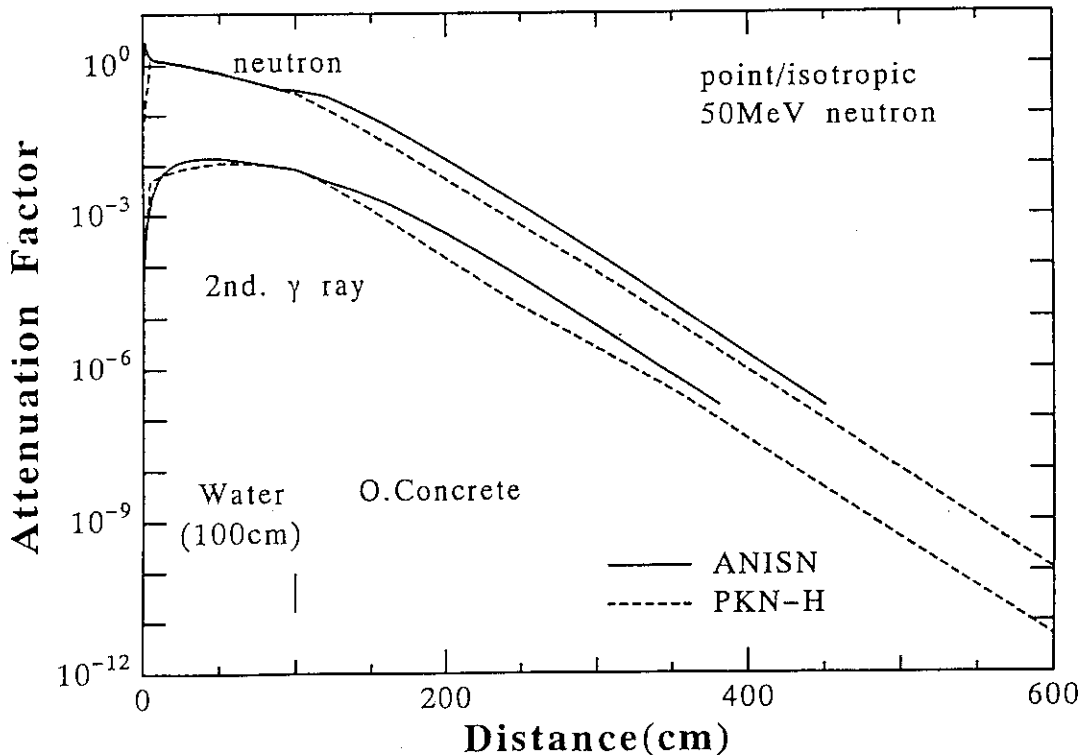


Fig. 2.2 Attenuation factor of neutron and secondary gamma ray dose equivalent for point isotropic 50MeV neutrons in water-concrete shield. —ANISN-JR, -PKN-H.

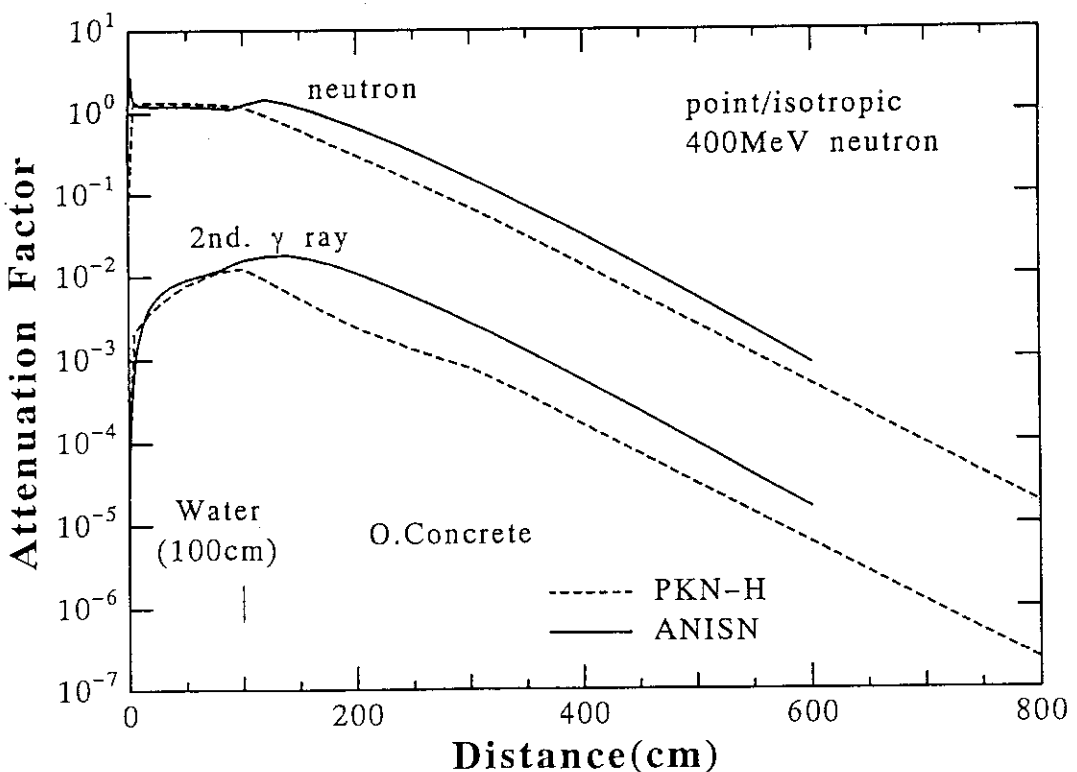


Fig. 2.3 Attenuation factor of neutron and secondary gamma ray dose equivalent for point isotropic 400MeV neutrons in water-concrete shield. —ANISN-JR, -PKN-H.

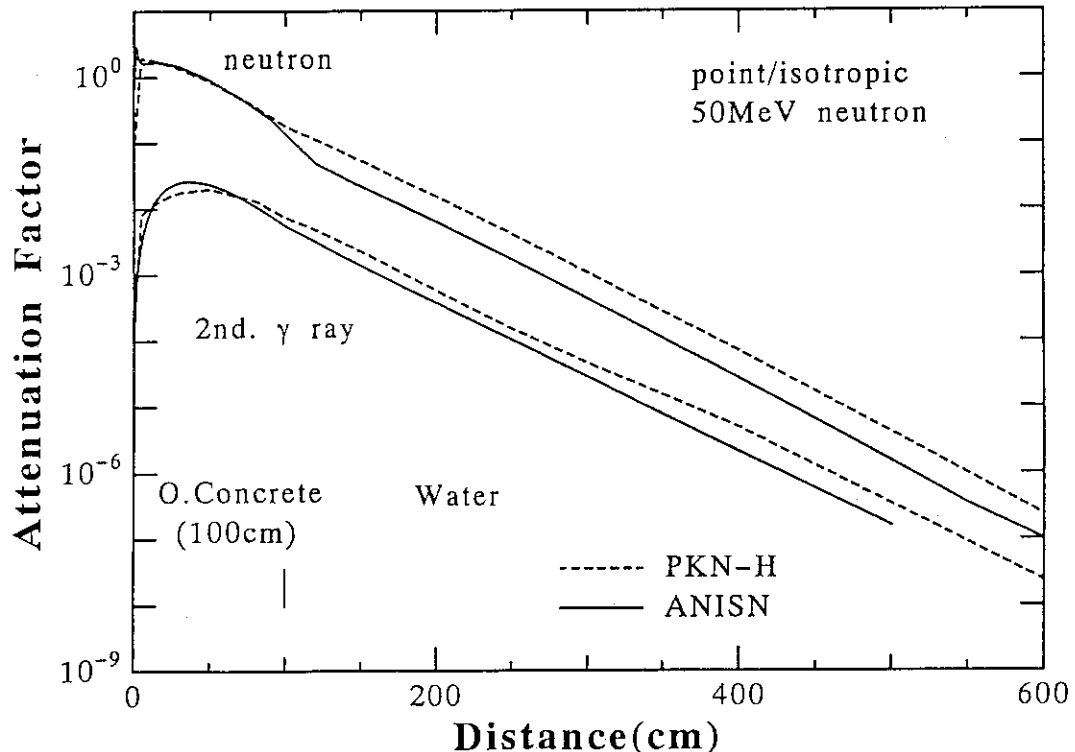


Fig. 2.4 Attenuation factor of neutron and secondary gamma ray dose equivalent for point isotropic 50MeV neutrons in water-iron shield. —ANISN-JR, -PKN-H.

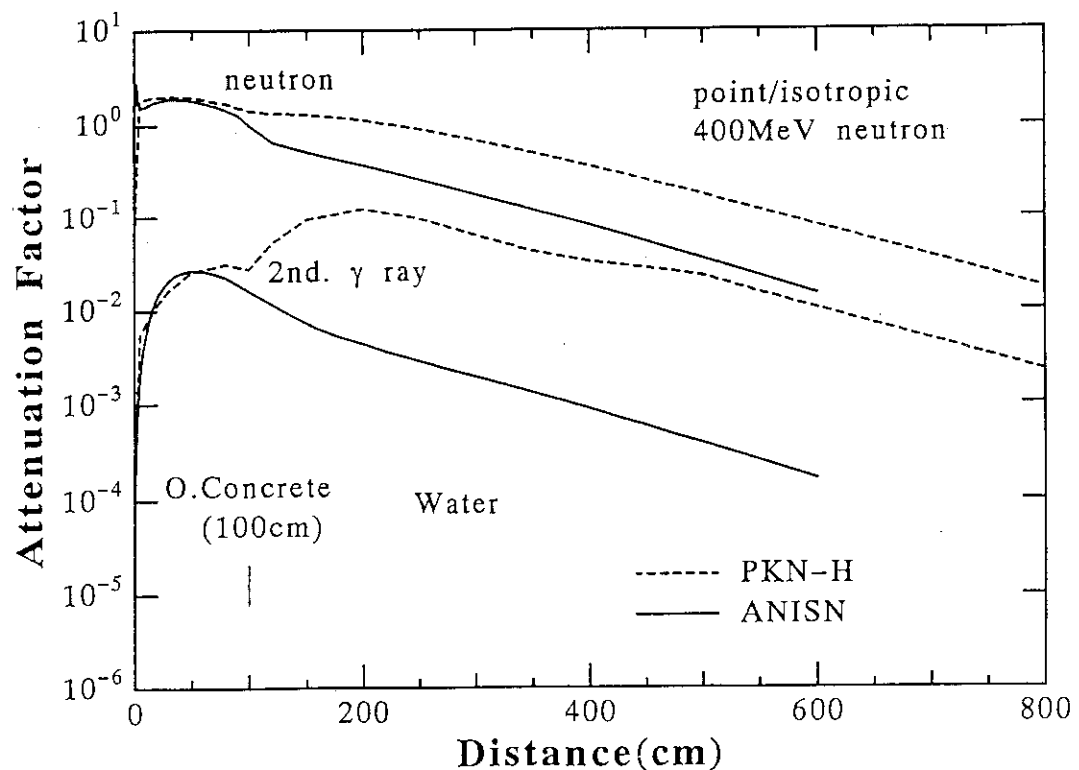


Fig. 2.5 Attenuation factor of neutron and secondary gamma ray dose equivalent for point isotropic 400MeV neutrons in water-iron shield. —ANISN-JR, -PKN-H.

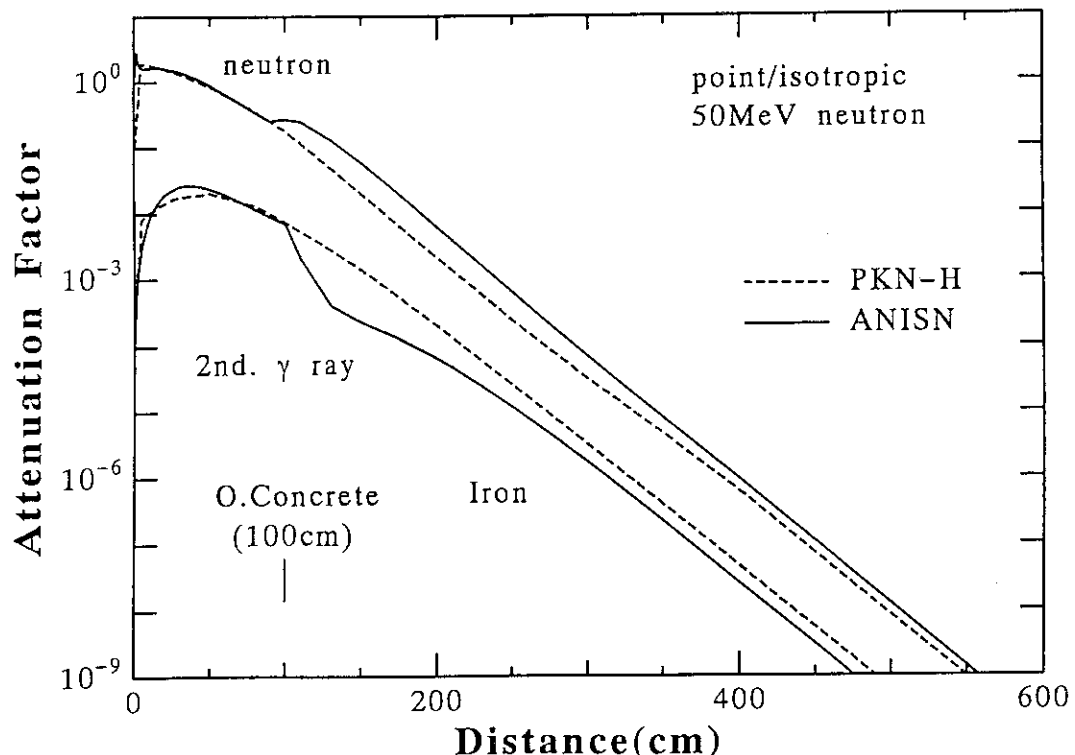


Fig. 2.6 Attenuation factor of neutron and secondary gamma ray dose equivalent for point isotropic 50MeV neutrons in iron-water shield. —ANISN-JR, -PKN-H.

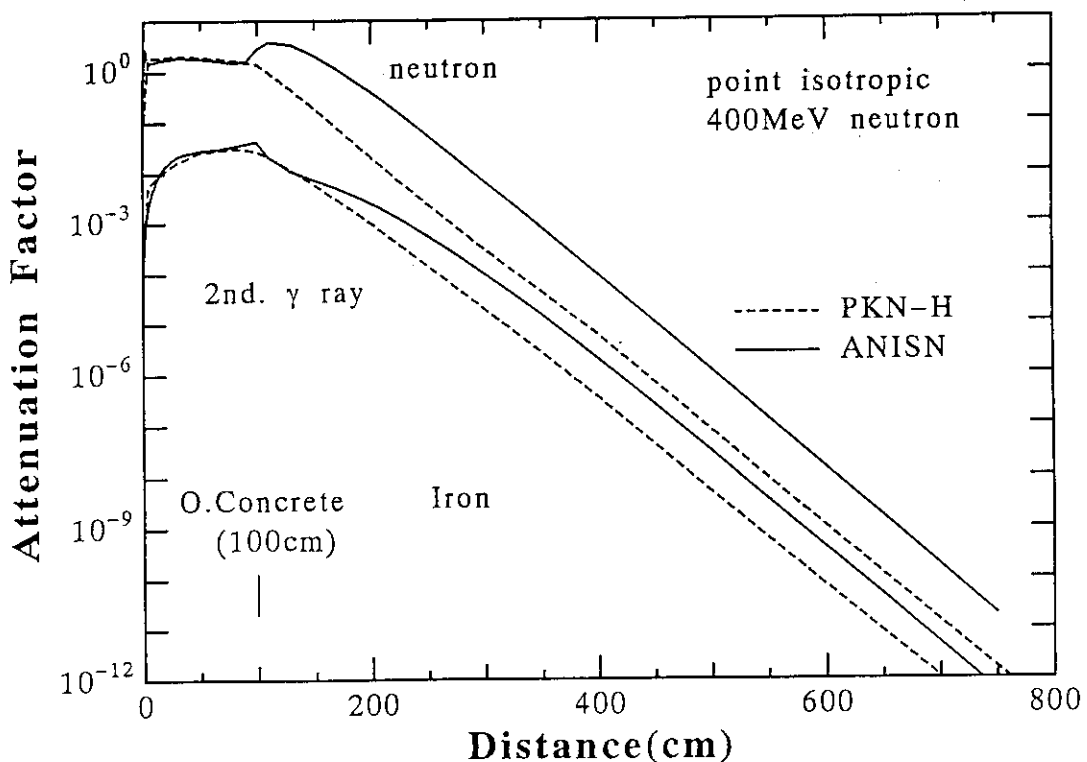


Fig. 2.7 Attenuation factor of neutron and secondary gamma ray dose equivalent for point isotropic 400MeV neutrons in iron-water shield. —ANISN-JR, -PKN-H.

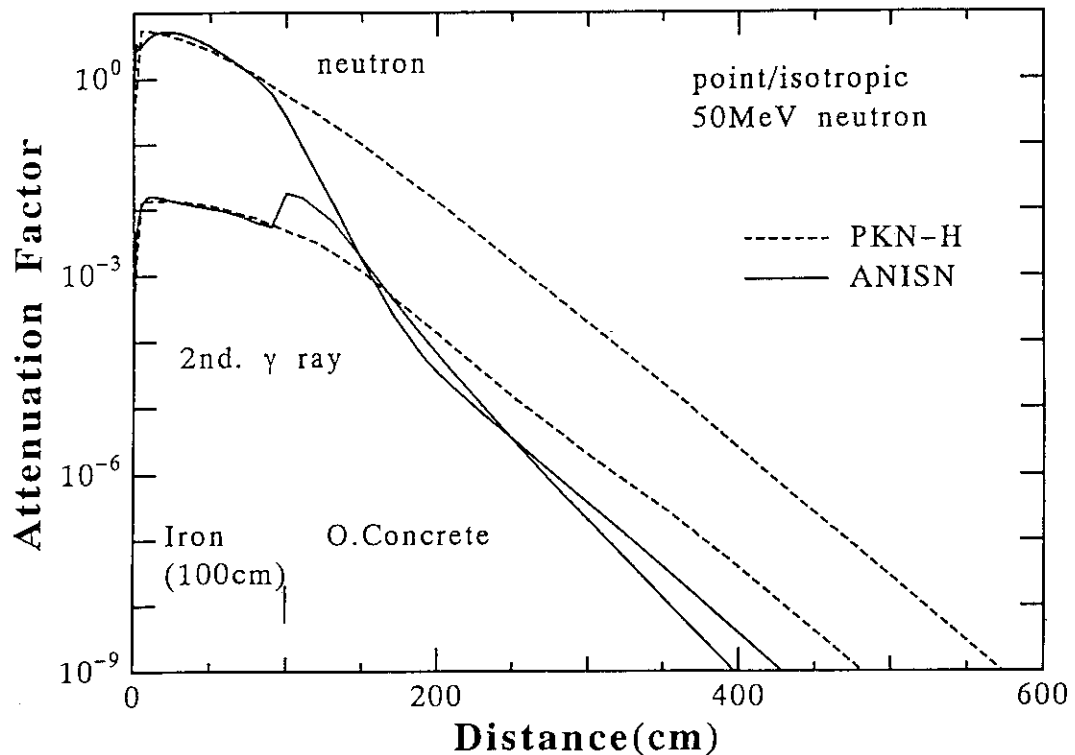


Fig. 2.8 Attenuation factor of neutron and secondary gamma ray dose equivalent for point isotropic 50MeV neutrons in iron-concrete shield. —ANISN-JR, -PKN-H.

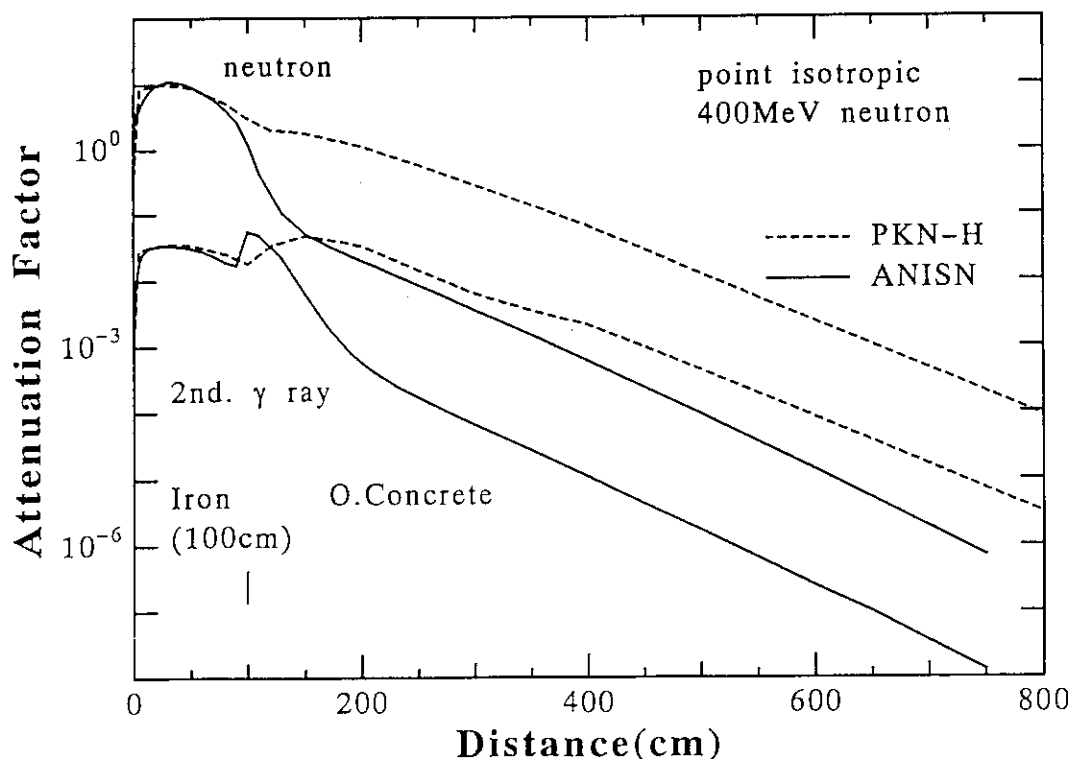


Fig. 2.9 Attenuation factor of neutron and secondary gamma ray dose equivalent for point isotropic 400MeV neutrons in iron-concrete shield. —ANISN-JR, -PKN-H.

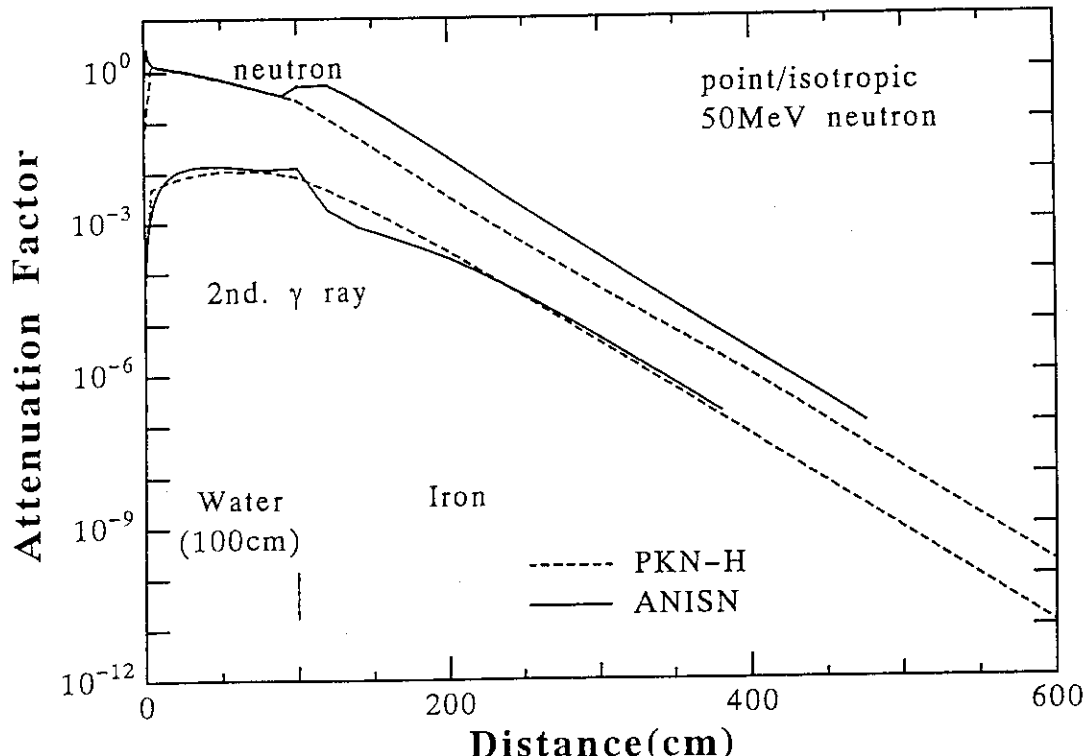


Fig. 2.10 Attenuation factor of neutron and secondary gamma ray dose equivalent for point isotropic 50MeV neutrons in concrete-water shield. —ANISN-JR, -PKN-H.

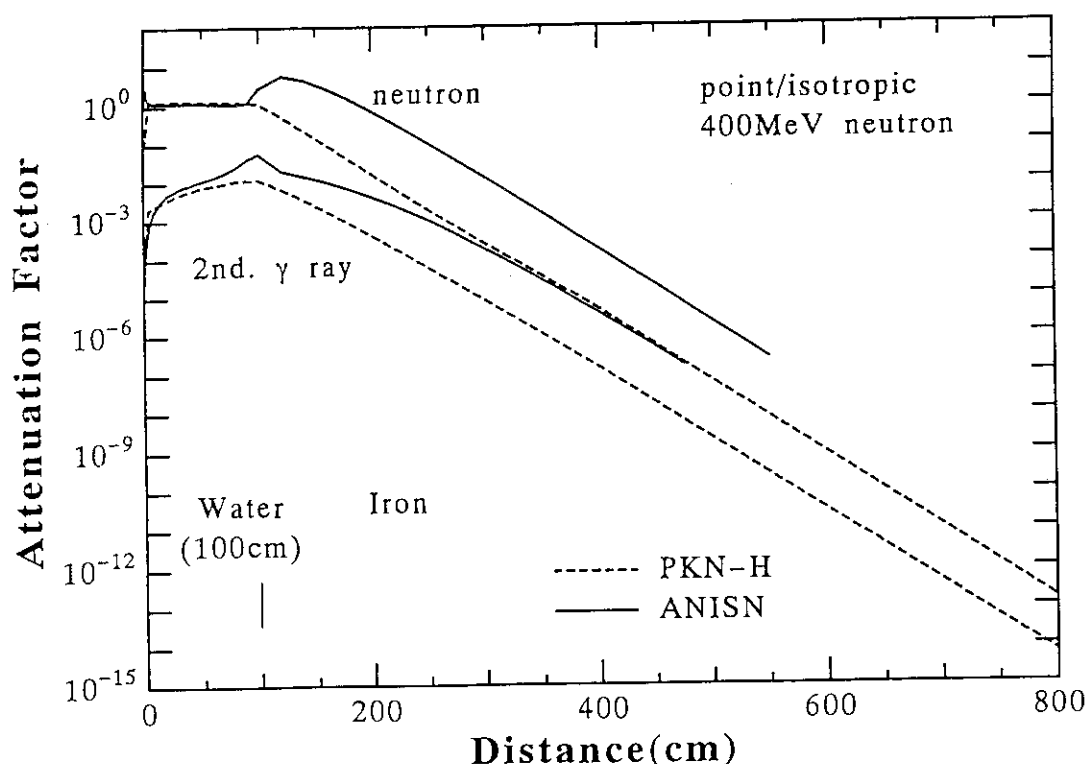


Fig. 2.11 Attenuation factor of neutron and secondary gamma ray dose equivalent for point isotropic 400MeV neutrons in concrete-water shield. —ANISN-JR, -PKN-H.

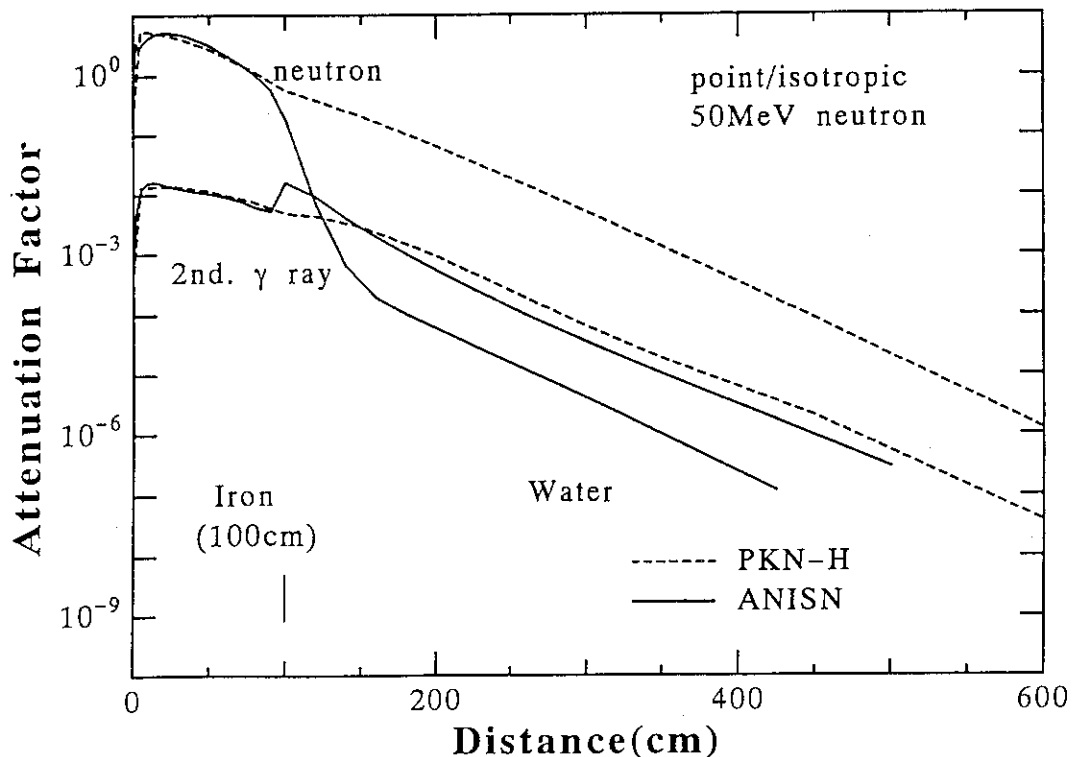


Fig. 2.12 Attenuation factor of neutron and secondary gamma ray dose equivalent for point isotropic 50MeV neutrons in concrete-iron shield. —ANISN-JR, -PKN-H.

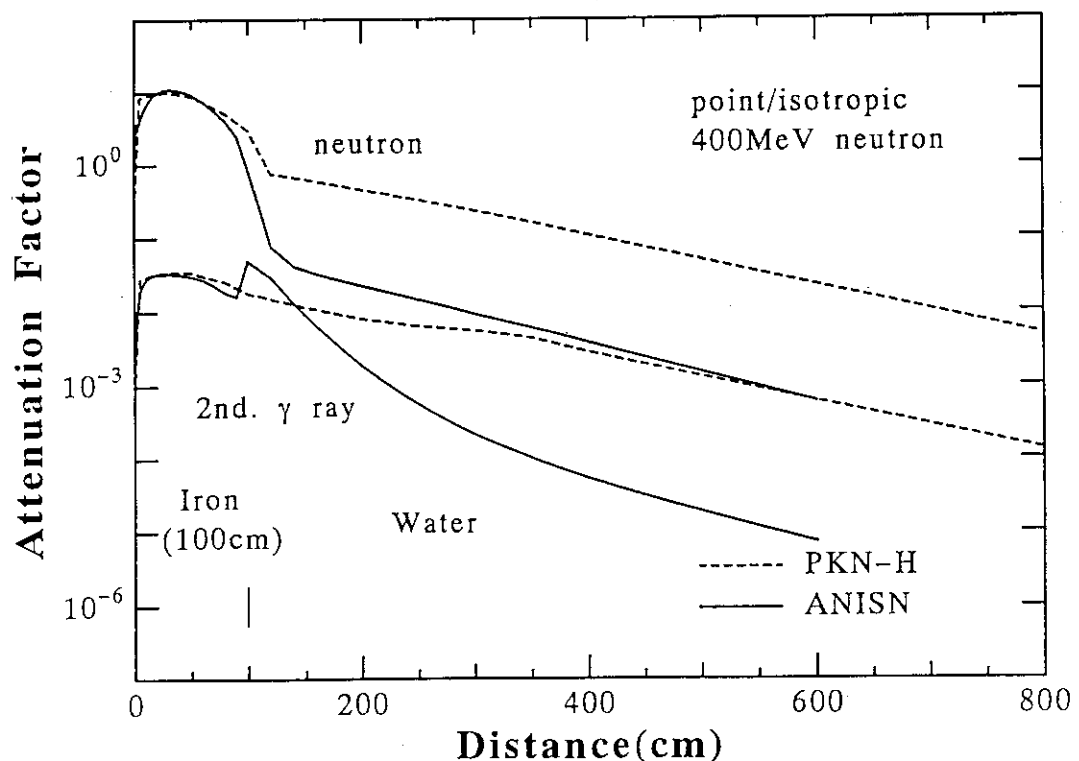


Fig. 2.13 Attenuation factor of neutron and secondary gamma ray dose equivalent for point isotropic 400MeV neutrons in concrete-iron shield. —ANISN-JR, -PKN-H.

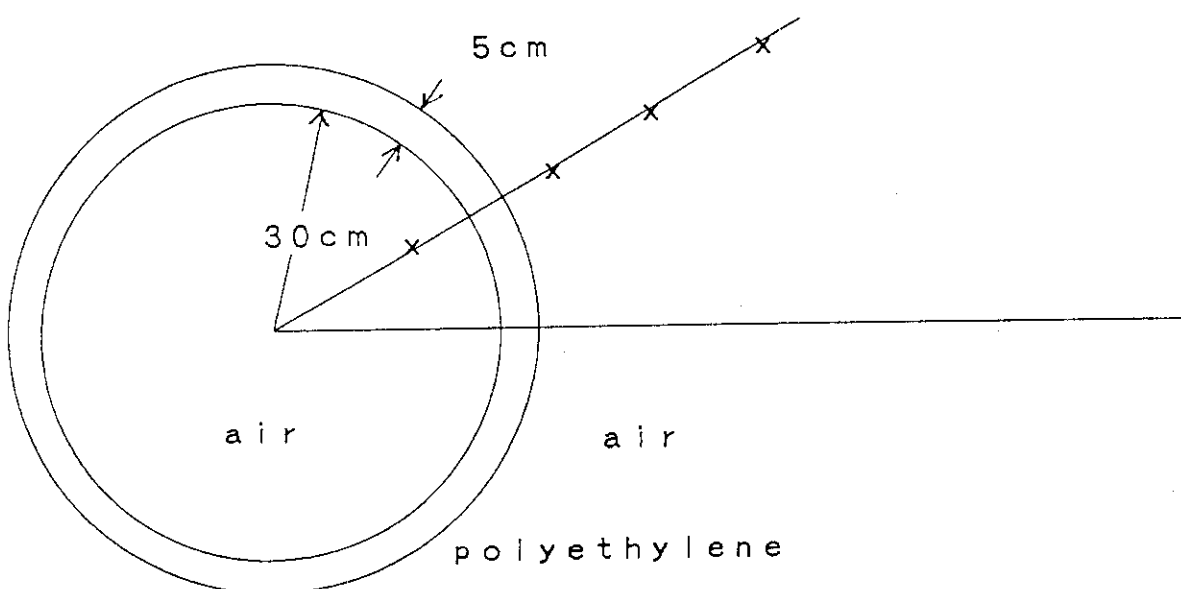


Fig. 3.1 Calculational model of sample problem 1.

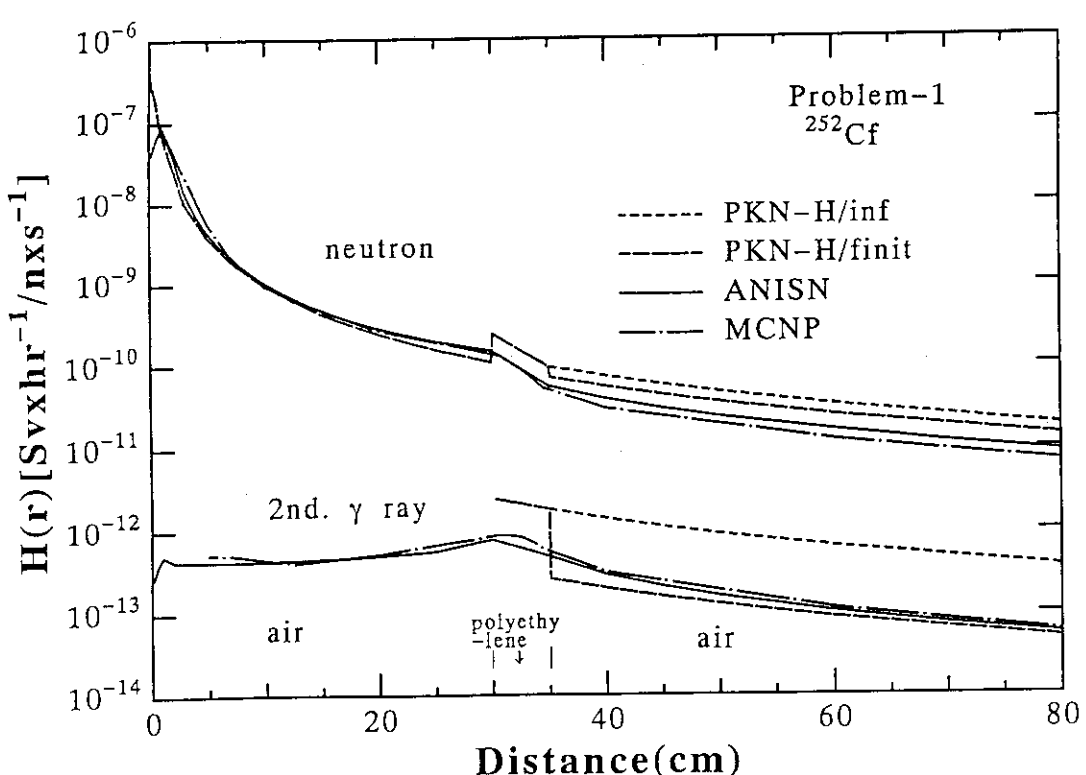


Fig. 3.2 Calculational results of neutron and secondary gamma ray dose equivalent for sample problem 1.

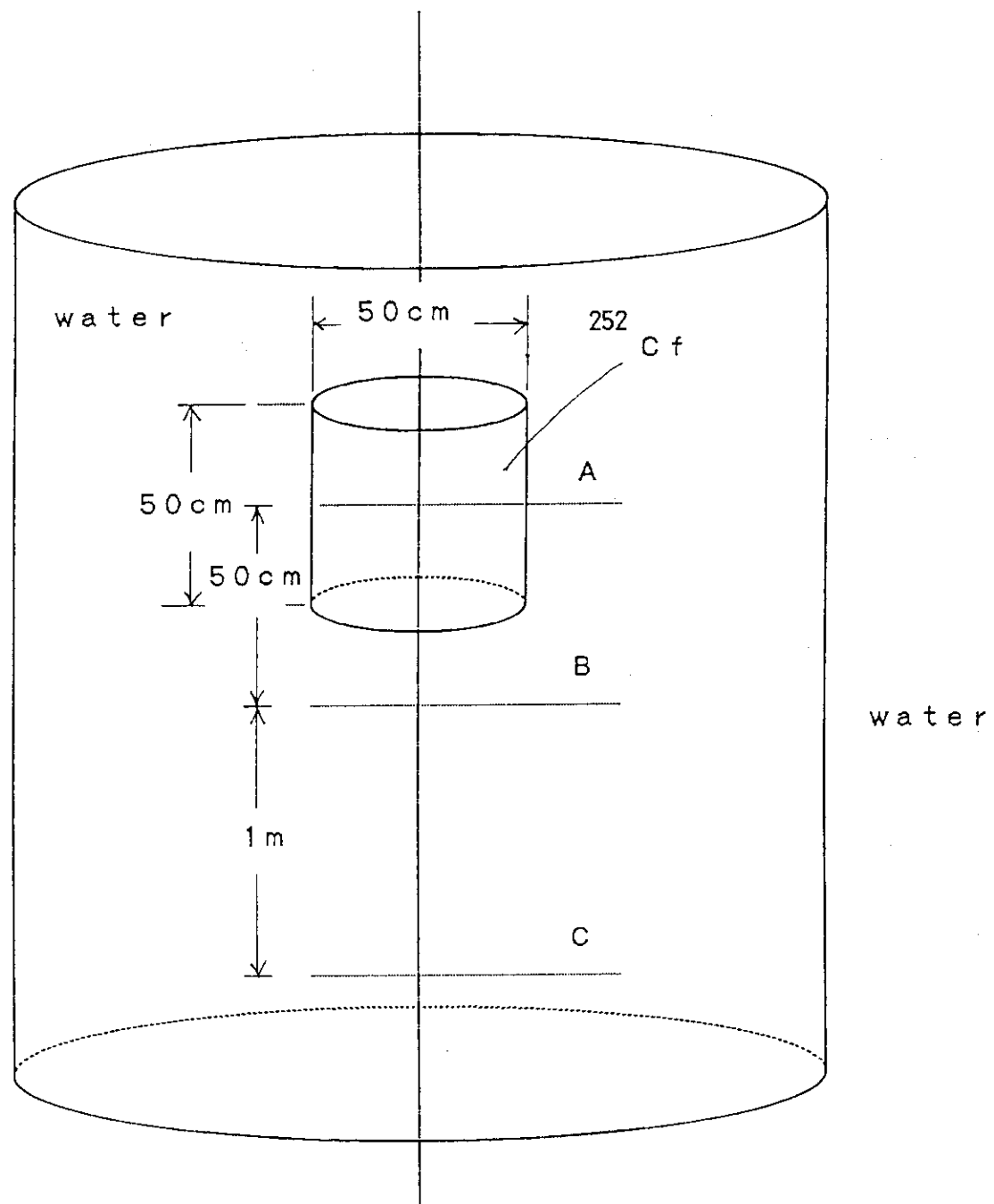


Fig. 3.3 Calculational model of sample problem 2.

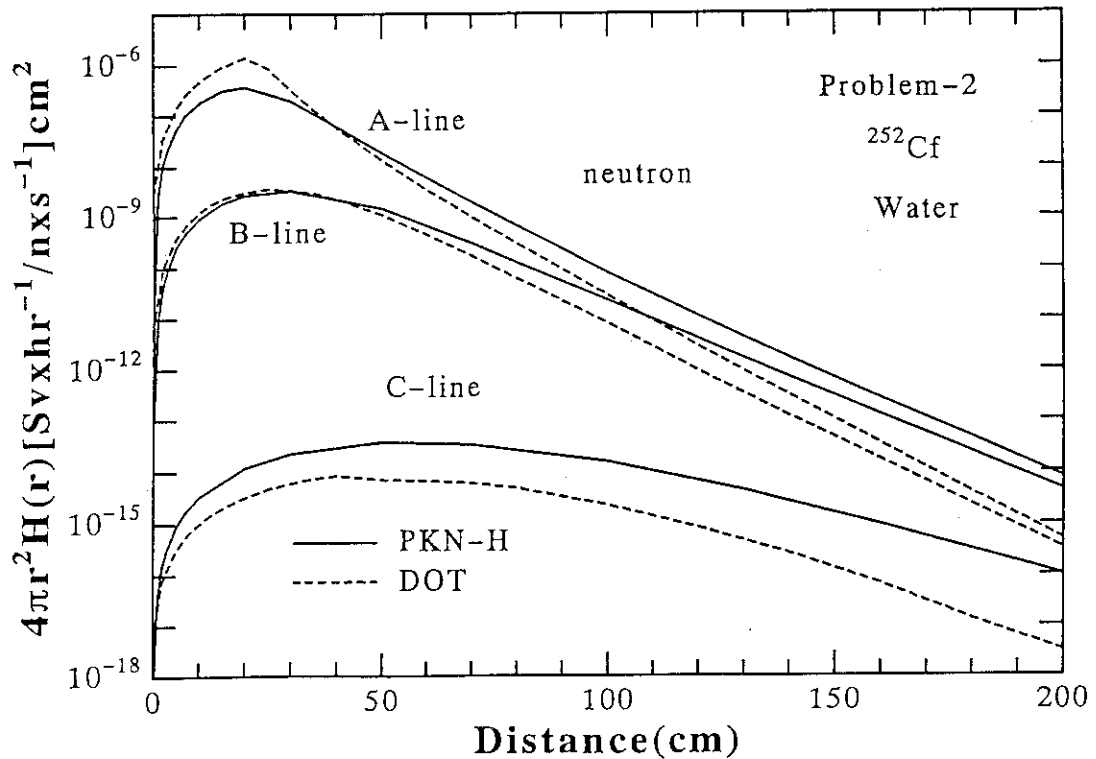


Fig. 3.4 Calculational result of neutron dose equivalent for sample problem 2.

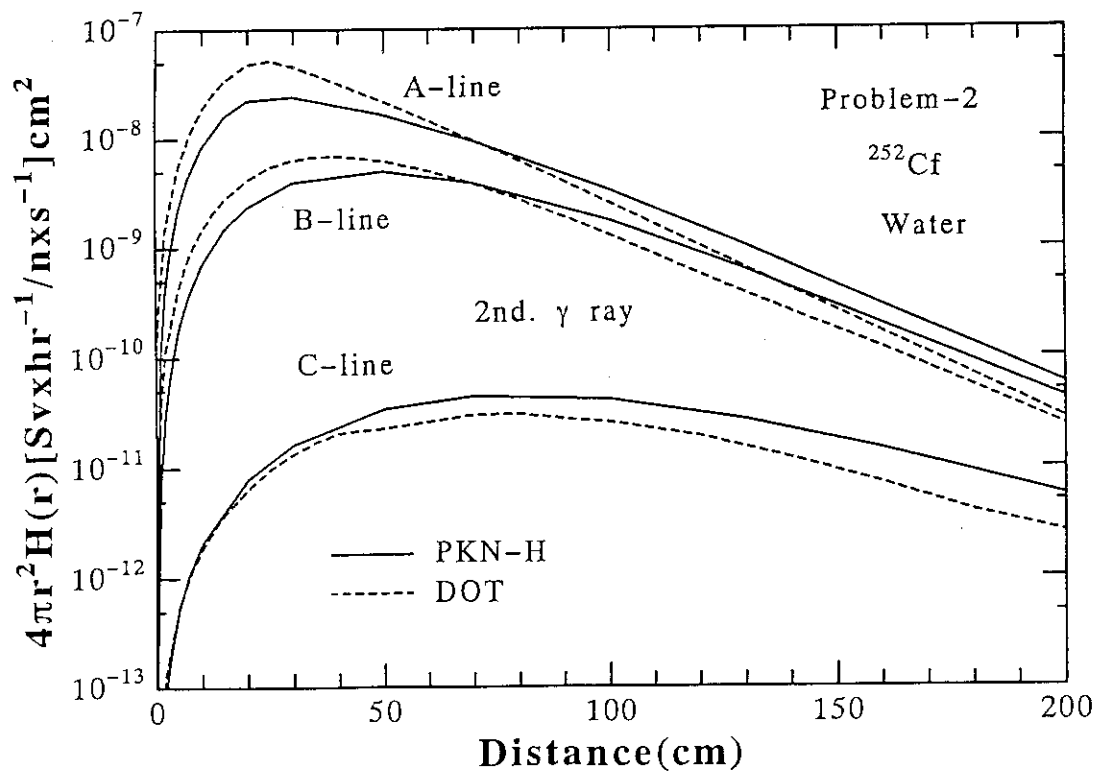


Fig. 3.5 Calculational result of secondary gamma ray dose equivalent for sample problem 2.

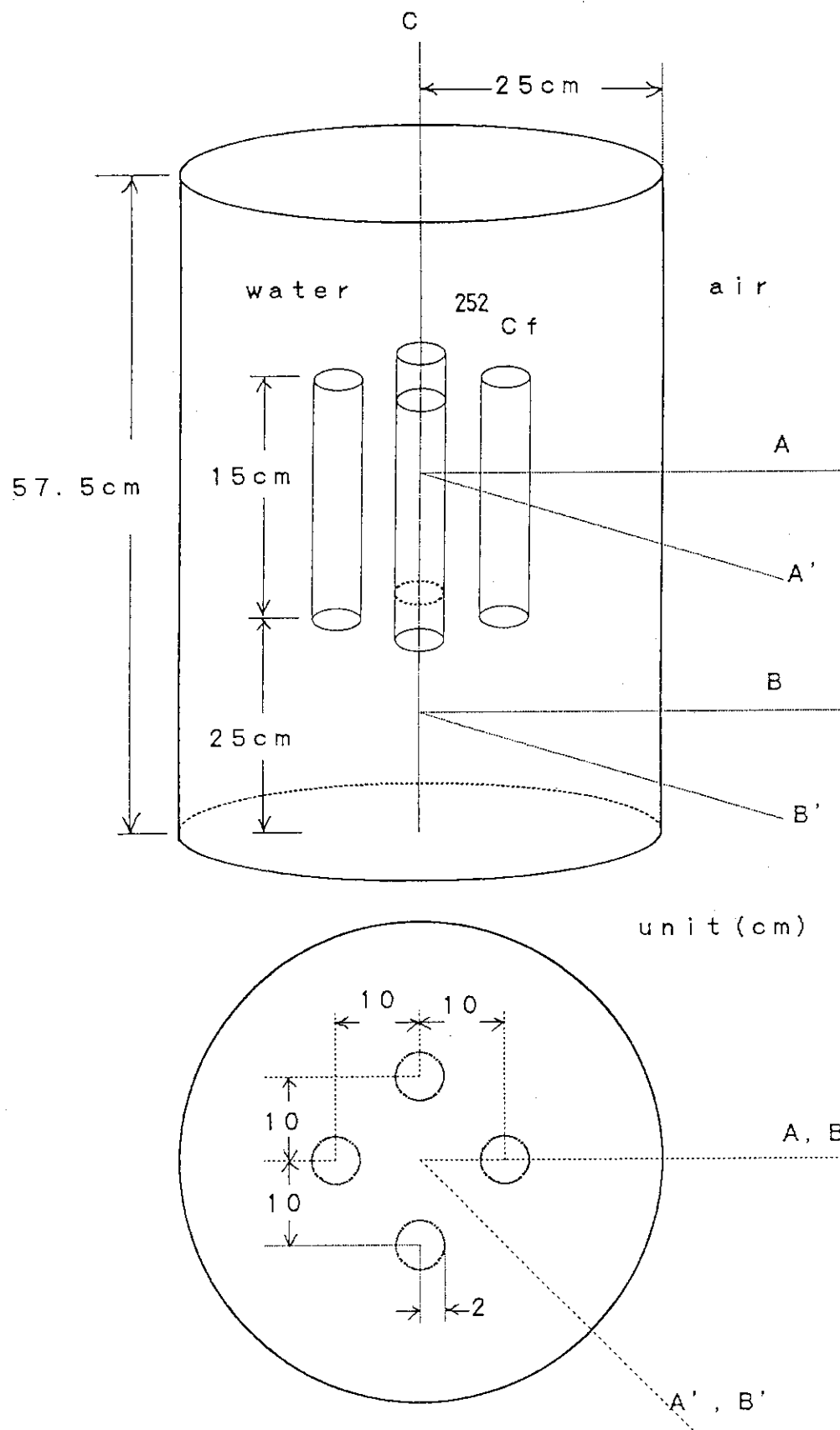


Fig. 3.6 Calculational model of sample problem 3.

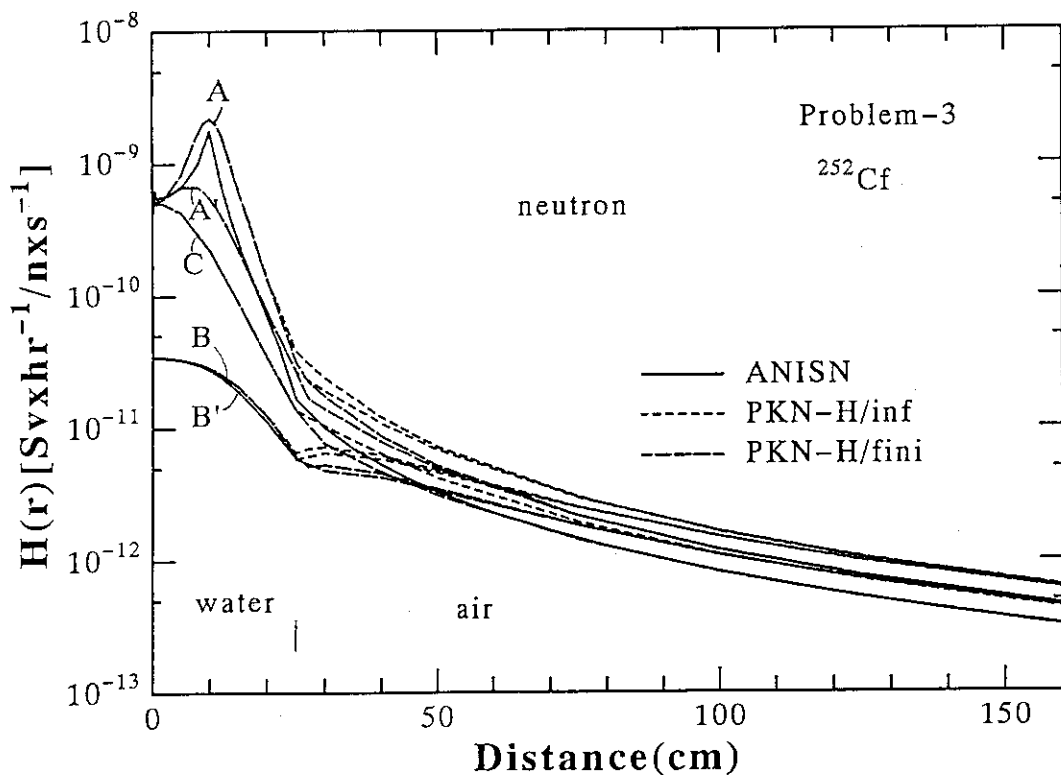


Fig. 3.7 Calculational results of neutron dose equivalent for sample problem 3.

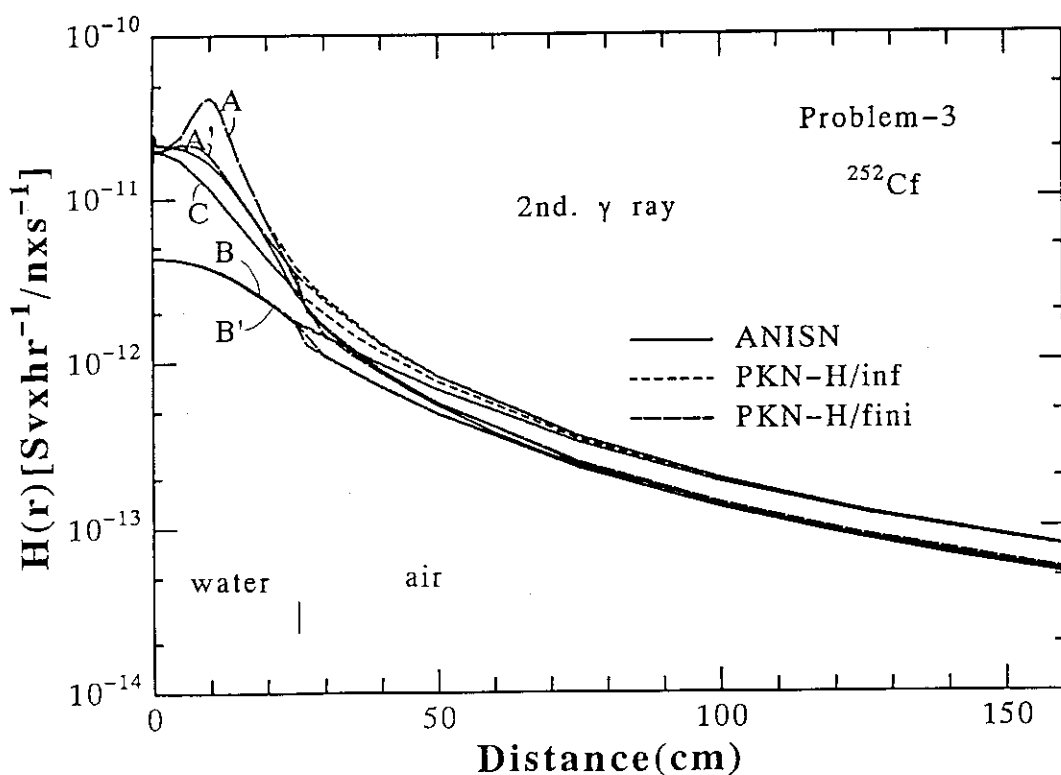


Fig. 3.8 Calculational results of secondary gamma ray dose equivalent for sample problem 3.

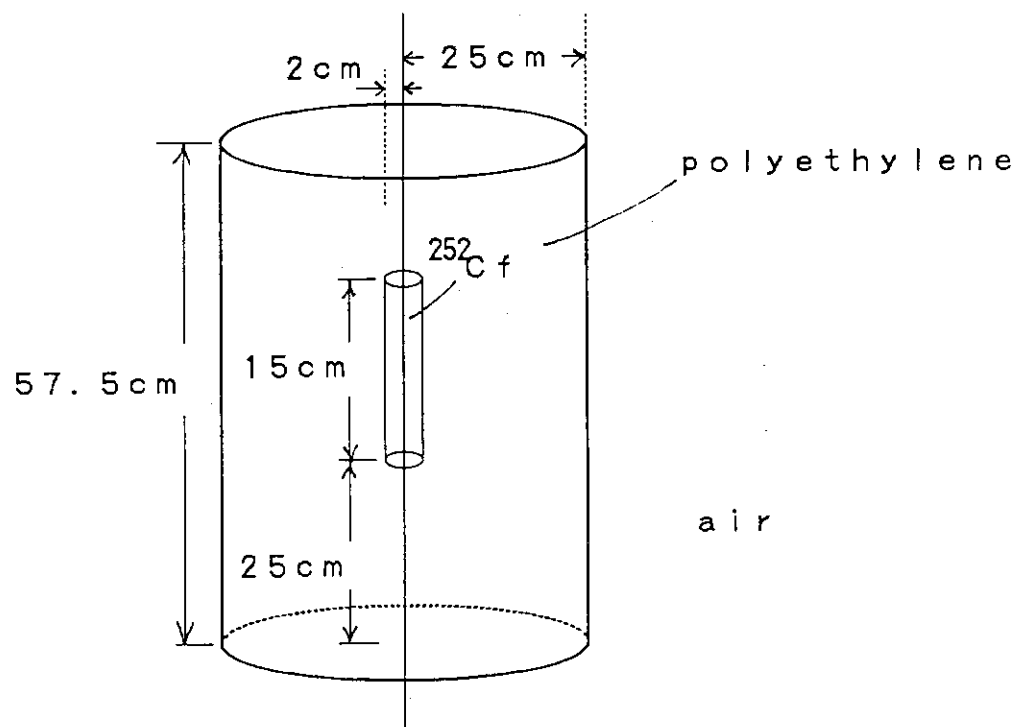
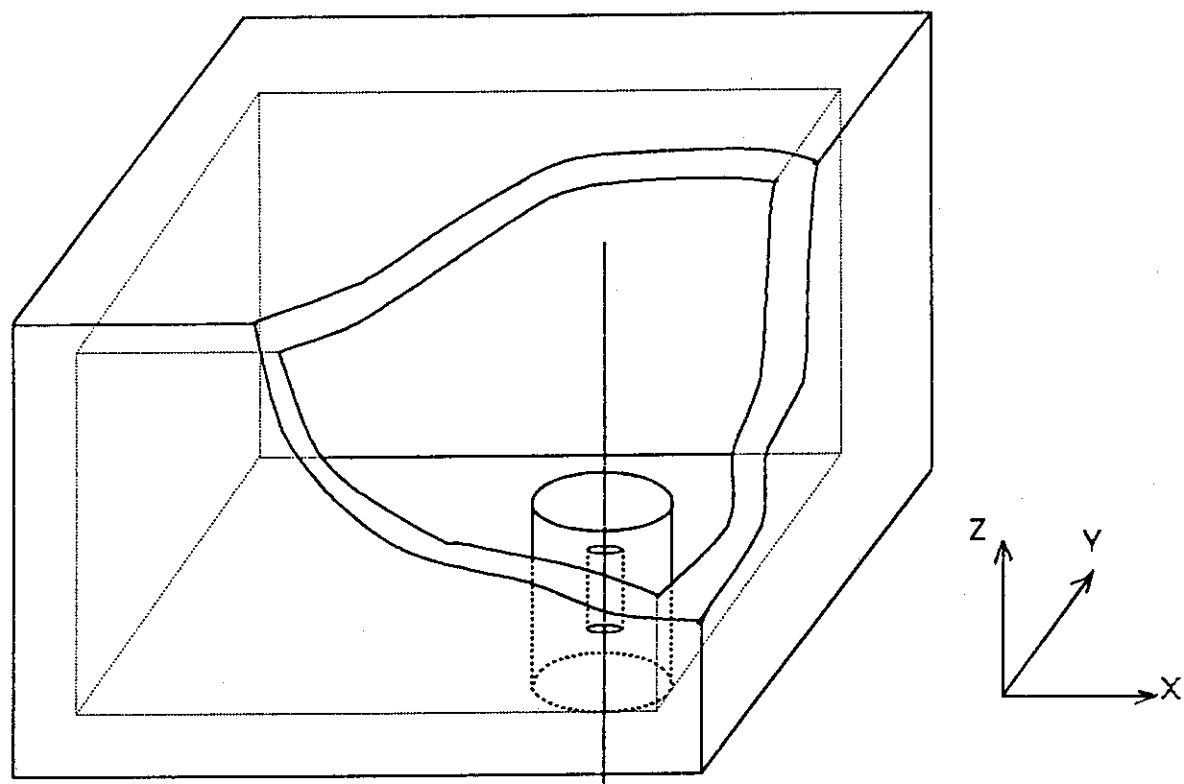


Fig. 3.9(1) Calculational model of sample problem 4.

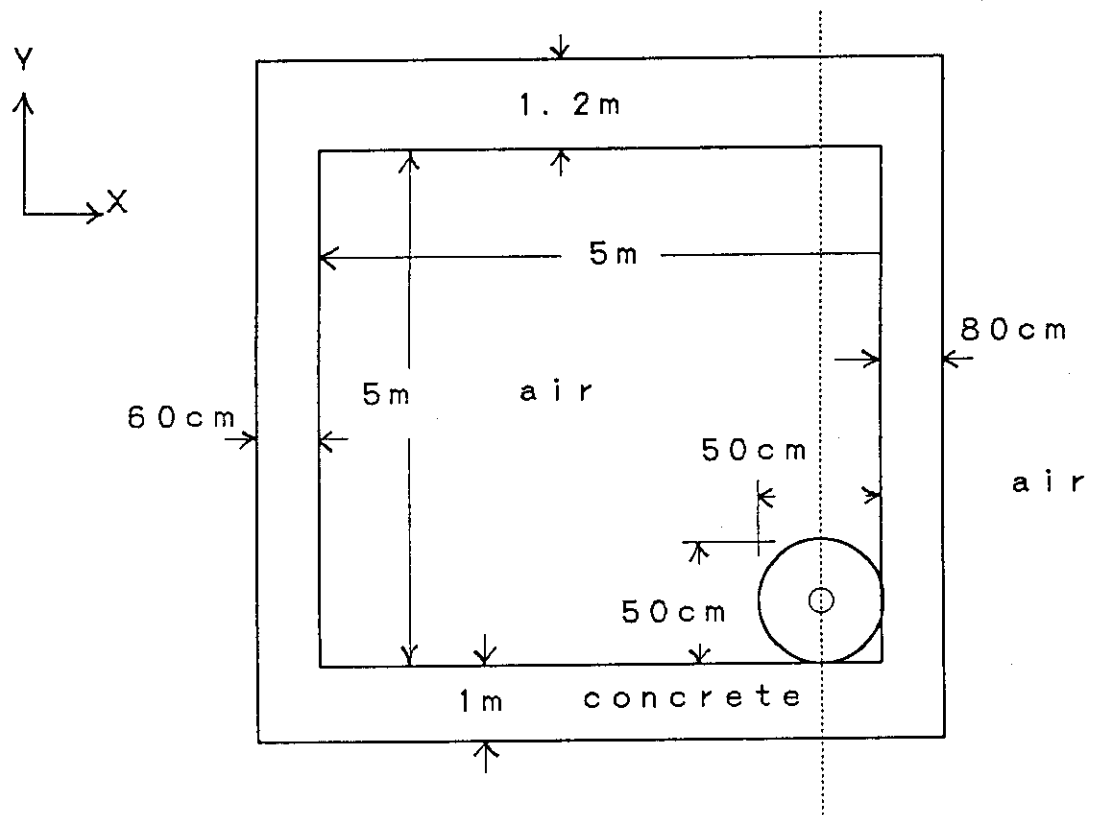
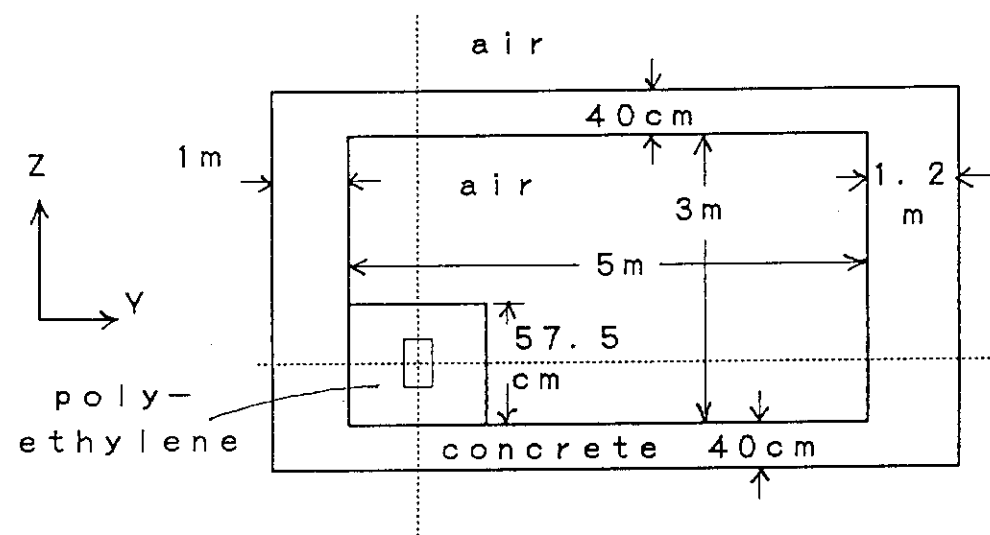


Fig. 3.9(2) Calculational model of sample problem 4.

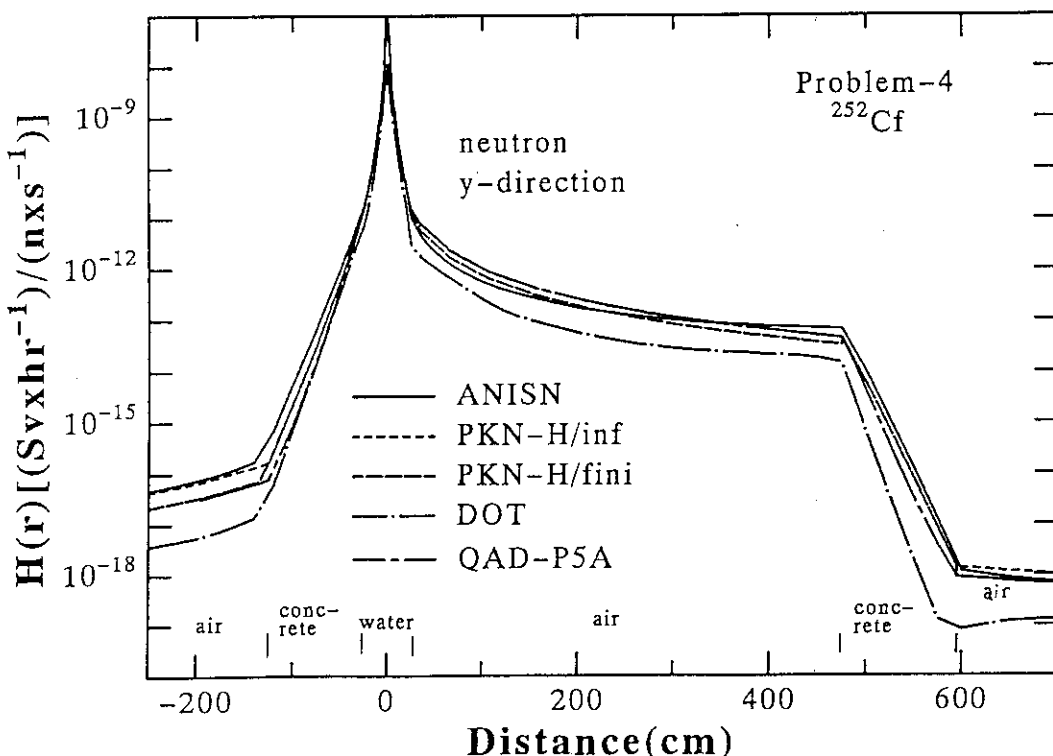


Fig. 3.10 Calculational results of neutron dose equivalent along y-direction for sample problem 4.

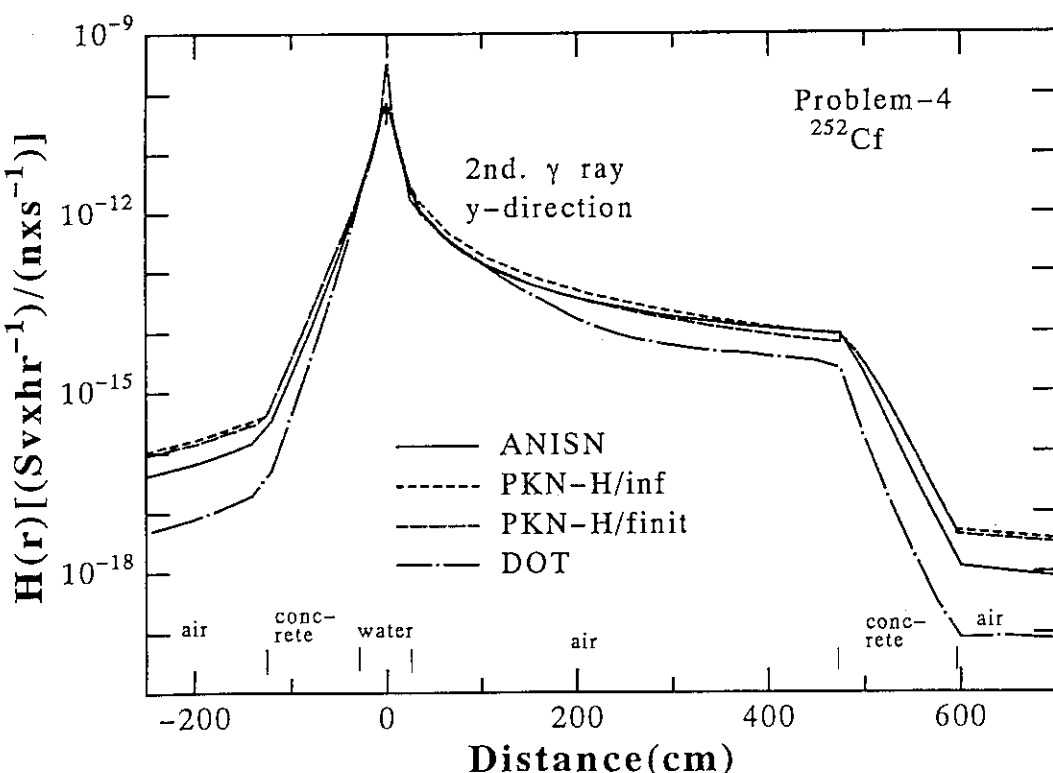


Fig. 3.11 Calculational results of secondary gamma ray dose equivalent along y-direction for sample problem 4.

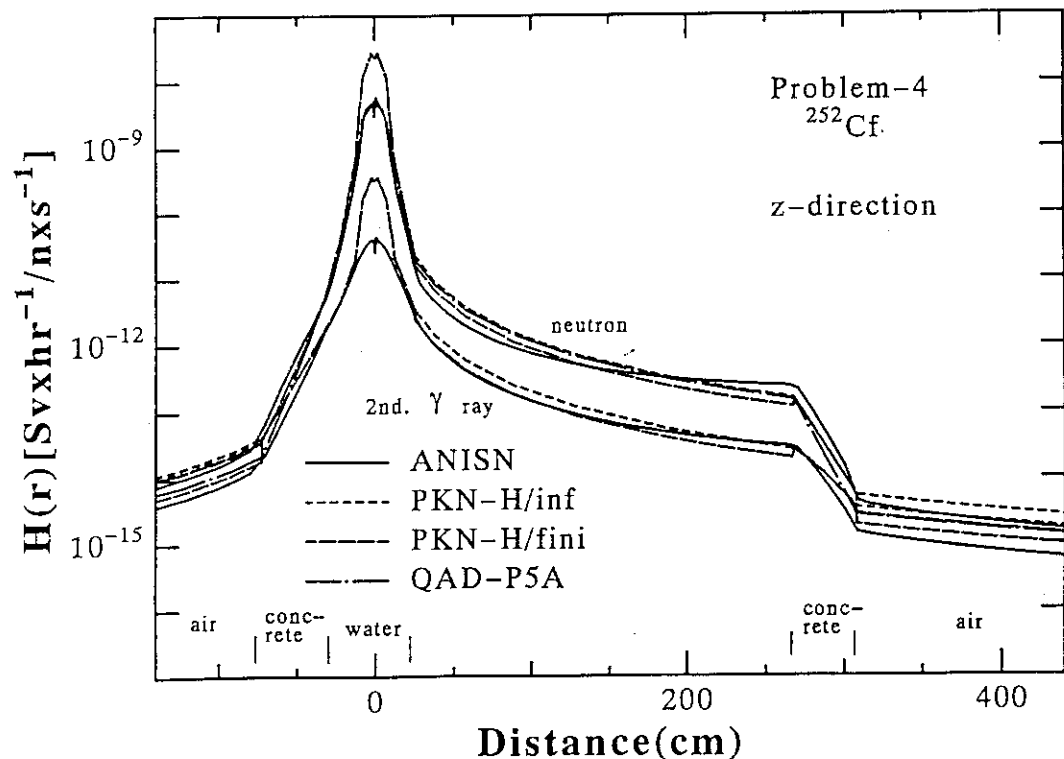


Fig. 3.12 Calculational results of neutron and secondary gamma ray dose equivalent along z-direction for sample problem 4.

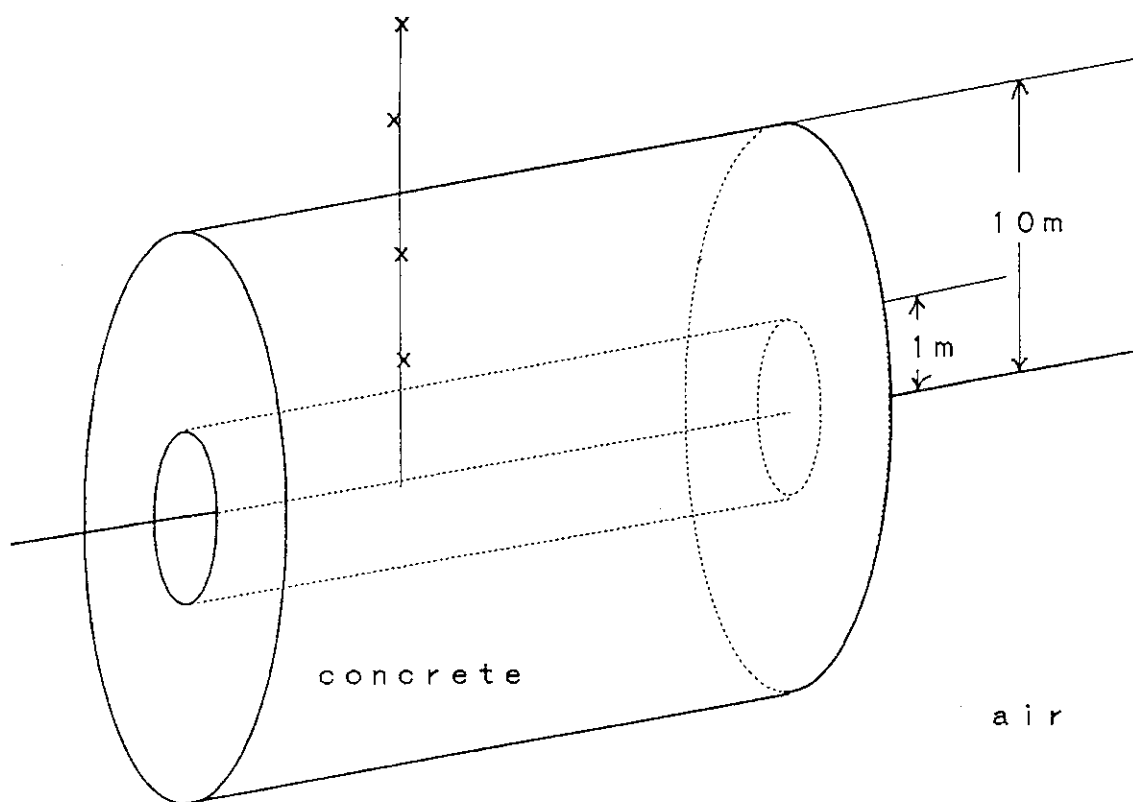


Fig. 3.13 Calculational model of sample problem 5.

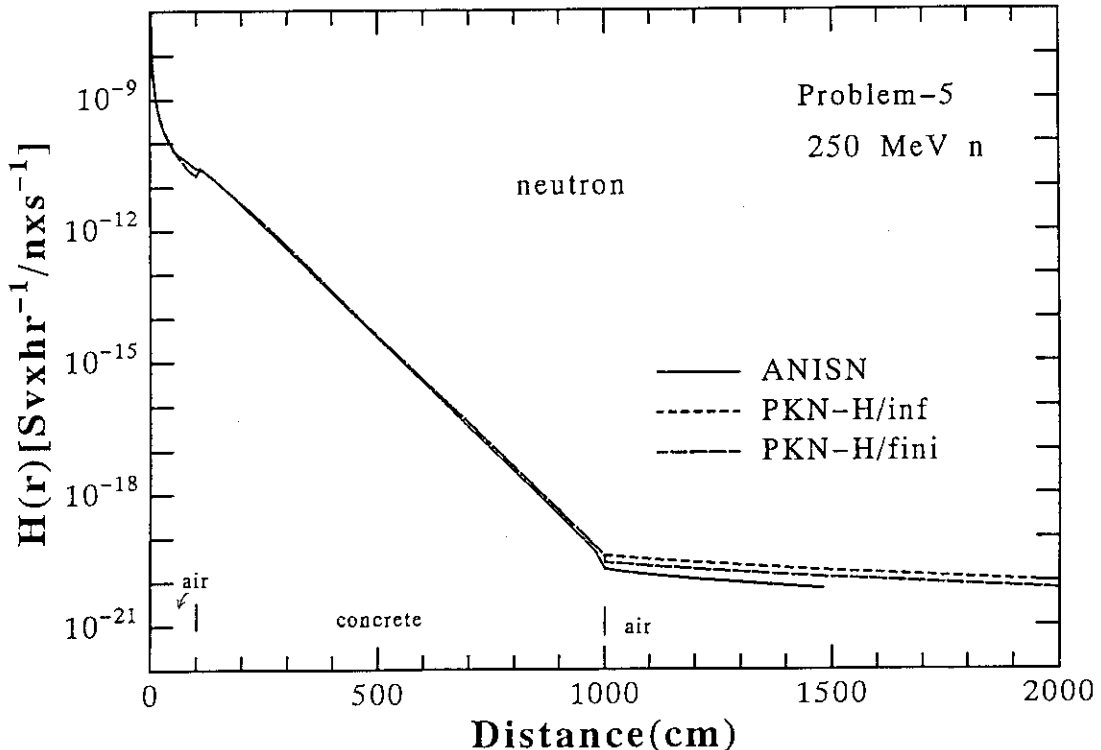


Fig. 3.14 Calculational results of neutron dose equivalent for sample problem 5.

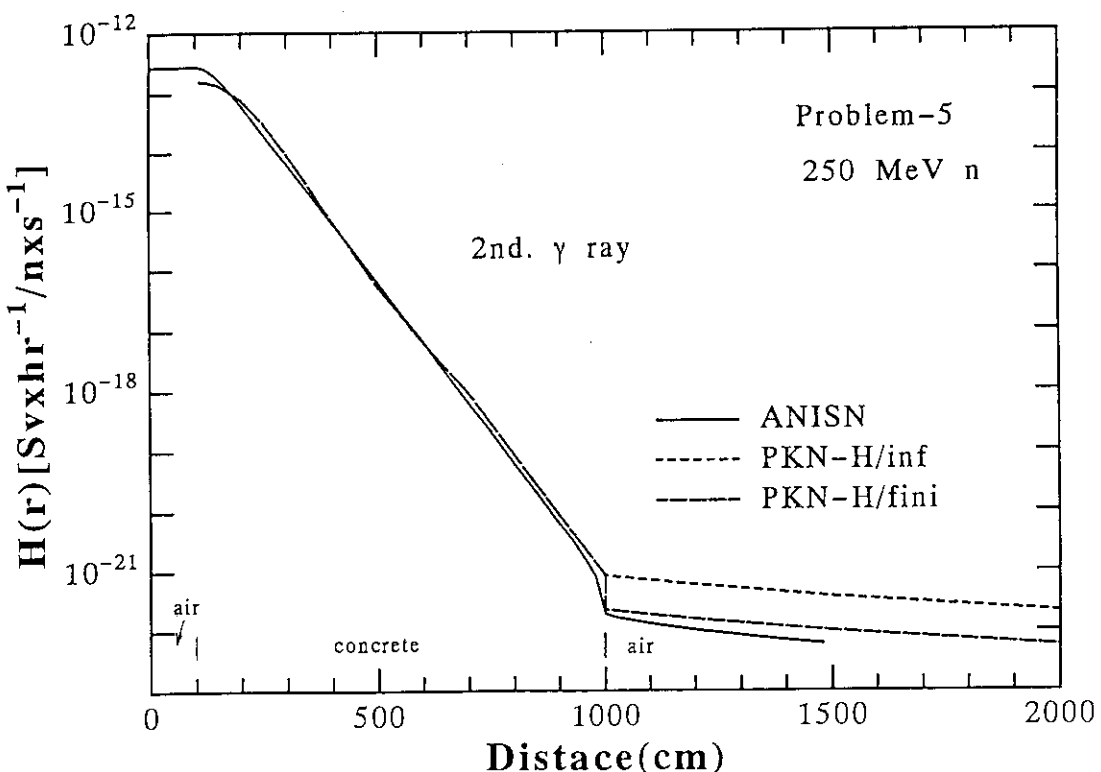


Fig. 3.15 Calculational results of secondary gamma ray dose equivalent for sample problem 5.

Appendix

A. 1	Input manual of PKN-H	31
A. 2	Input data of sample problem 1	36
A. 3	Input data of sample problem 2	37
A. 4	Input data of sample problem 3	39
A. 5	Input data of sample problem 4	42
A. 6	Input data of sample problem 5	44
A. 7	Output	46
A. 8	Output data of sample problem 1	46
A. 9	Output data of sample problem 2	47
A. 10	Output data of sample problem 3	49
A. 11	Output data of sample problem 4	51
A. 12	Output data of sample problem 5	53
A. 13	Energy spectrum of ^{252}Cf fission and ^{241}Am -Be neutrons	54
A. 14	Flux to dose equivalent conversion factor of neutrons	55
A. 15	Flux to dose equivalent conversion factor of gamma rays	56
A. 16	Input required on CGB cards for each body type	57
A. 17	Description of body types	58
A. 18	Infinite medium effect for ^{252}Cf fission and ^{241}Am -Be neutrons	63

Appendix A.1 Input manual of PKN-H.

It is necessary to prepare CARD-A to CARD-Z. The cartesian, spherical or cylindrical geometries are available, each 3-dimensional coordinates are expressed, generally, X1, X2 and X3. Three axes correspond X, Z and Y in the cartesian coordinates and R, Θ and Ψ in spherical coordinates and R, Z and Θ in the cylindrical coordinates, respectively.

CARD-A (A72); Title

CARD-B (14I4);

NSX1 : total number of input location of X1 coordinate of source

NSX2 : total number of input location of X2 coordinate of source

NSX3 : total number of input location of X3 coordinate of source

NREG : total number of regions(or zones) defined in CARD-CGC

NBOD : total number of bodies defined in CARD-CGB

NSOPT : coordinates system described the form of source

(0/1/2)=(Cylindrical/Cartesian/Spherical coordinates)

ISRC : Type of source

(0/1/2)=(source of the previous case is used/cosine-

distributed source is used/source is computed using the
weighting values input along each coordinate axis)

CARD-C (E10.3,6I5) ;CID00,((CID(I,J),I=1,2),J=1,3)

CID00 : The total source strength in fissions/sec, Captures/sec,
or decays/sec. (default = 1)

CID : Constants for cosine source distribution.

(CID is ignored, if ISRC does not equal to 1.)

If ISRC equals 1, Source strength distribution is calculated
as following equation,

Source strength(X1,X2,X3)=CID00*COS(CID(1,1)*(X1-CID(2,1))
COS(CID(1,2)(X2-CID(2,2)))
COS(CID(1,3)(X3-CID(2,3))).

CARD-D (8E9.2) ;(SOX1(I),I=1,NSX1+1)

SOX1 : Coordinates of source volume divisions along X1-axis.

CARD-E (8E9.2) ;(SOX2(I),I=1,NSX2+1)

SOX2 : Coordinates of source volume divisions along X2-axis.

CARD-F (8E9.2) ;(SOX3(I),I=1,NSX3+1)

SOX3 : Coordinates of source volume divisions along X3-axis.

Note: Source intensity is normalized to 1.

CARD-G (3E9.2,I9,E9.2) ; TSX1(I),TSX2(I),TSX3(I),ITS(I),WTS(I)

TSX1 : Center coordinate of I-th source volume along X1-axis.

TSX2 : Center coordinate of I-th source volume along X2-axis.

TSX3 : Center coordinate of I-th source volume along X3-axis.

ITS : Coordinate system describing center coordinates

(0/1/2)=(Cylindrical/Cartesian/Spherical coordinates)

WTS : Weight(ratio) of I-th source volume

Note: CARD-G iterates numbers of source blocks, if source separates
into more than two blocks.

Note: I-th source coordinates is calculated, as follows,

(SOX1+TSX1(I),SOX2+TSX2(I),SOX3+TSX3(I))

CARD-H (I36) ;ITSH

ITSH : ITSH=-2 means end of CARD-G data.

If ISRC dose not equal to 2, CARD-I, -J and -K are not necessary.

CARD-I (8E9.2) ; (SWX1(I),I=1,NSX1+1)

SWX1 : Weight of source strength for source location SOX1.

CARD-J (8E9.2) ; (SWX2(I),I=1,NSX2+1)

SWX2 : Weight of source strength for source location SOX2.

CARD-K (8E9.2) ; (SWX3(I),I=1,NSX3+1)

SWX3 : Weight of source strength for source location SOX3.

For combinatorial geometry input data, next CARD-CGA to CARD-CGE should be prepared.

CARD-CGA (2I5,10X,10A6)

IVOPT : Set to zero for PKN-H input.

IDBG : set to zero for PKN-H input.

JTY : alphanumeric title for geometry input (columns 21-80)

CARDs-CGB (2X,A3,1X,I4,6D10.3)

One set of CGB cards is required for each body and for the END card. (see Appendix A.16). Leave columns 1-6 blank on all continuation cards.

ITYPE : specifies body type or END to terminate reading of body and (for example BOX, RPP, ARB, etc.). Leave blank for continuation cards.

IALP : body number assigned by user (all input body numbers must form a sequence set beginning at 1). If left blank, numbers are assigned sequentially. Either assign all or none of the numbers. Leave blank for continuation cards.

FPD(I) : real data required for the given body as shown in Appendix A.16. This data must be in cm.

CARDs-CGC (2X,A3,I5,9(A2,I5))

Input zone specification cards. One set of cards required for each input zone, with input zone numbers being assigned sequentially.

IALP : IALP must be a nonblank for the first card of each set of cards defining an input zone. If IALP is blank, this card is treated as a continuation of the previous zone card.

IALP = END denotes the end of zone description.

NAZ : total number of zones that can be entered upon leaving any of the bodies defined for this input region (some zones may be counted more than once). Leave blank for continuation cards for a given zone. (If NAZ < 0 on the first card of the zone card set, then it is set to 5). This is used to allocate blank common.

Alternate IIBIAS(I) and JTY(I) for all bodies defining this input zone.

IIBIAS(I): specify the "OR" operator if required for the JTY(I) body.

JTY(I): body number with the (+) or (-) sign as required for the zone description.

CARDs-CGD (14I5)

MRIZ(I): MRIZ(I) is the region number in which the "Ith" input zone is contained(I = 1, to the number of input zones).

Region numbers must be sequentially defined from 1.

Number 1 region should be a region including source.

CARDs-CGE (14I5)

MMIZ(I): MMIZ(I) is the medium number in which the "Ith" input zone is contained(I = 1, to the number of input zones).

Medium numbers must be sequentially defined from 1 to 3, else 0 for external void, or 1000 for internal void.

CARD-S (3I5,2E9.2) ; IPP,IPD(1),IPD(2),PD6A,PD6B

IPP : ID number of energy dependence of source.

(1-6)=(1:mono energy/2:spread energy/3: ^{235}U /4: ^{252}Cf /5: ^{241}Am -Be
/6:Watt formula)

IPD(1) : First group of input of source group information (-1~59)

IPD(2) : Last group of input of source group information (-1~59)

PD6A : not need if IPP is not 6.

PD6B : not need if IPP is not 6.

If IPP=6, source strength is calculated according to the following equation,

$$S(E) \sim \exp(-PD6A \times E) \times \sinh(\sqrt{2} \times PD6B \times E)$$

E : source neutron energy(MeV).

CARDs-T (8E9.3) ; (QID(I), I=1, IPD(2)-IPD(1)+1)

QID(I) : The IPD(2)-IPD(1)+1 relative source strengths from IPD(1) to IPD(2) is necessary, if IPP=2.

This card is not necessary when IPD(2) is larger than IPD(1).

This card is ignored when IPP=6.

CARDs-X (3E9.3,I9); (RX1(I),RX2(I),RX3(I),NGM(I),I=1,NDET(≤ 100))

RX1 : Calculational coordinates along X1-axis.

RX2 : Calculational coordinates along X2-axis.

RX3 : Calculational coordinates along X3-axis.

NGM : Coordinates system describing detector point
(0/1/2)=(Cylindrical/Cartesian/Spherical coordinates)

CARD-X is necessary to iterate by number of detector points, NDET.

CARD-Z (33x,I3) ; IZT

IZT ==1 ; The end of input data.

Appendix A.2 Input data of sample problem 1.

	1	2	3	4	5	6	7	8
PKN-H-CG SPHERICAL GEOM.			252CF(POINT) SOURCE SPHERIC WAT /PKN-H/SP01/				CARD A	
1 1 2 3 3 0 1 2							CARD B	
1.0 0.0 0.0 0.0 0.0 0.0 0.0 0.0							CARD C	
0.0 1.0							CARD D	
-0.5 0.5							CARD E	
0.0 3.142 6.283							CARD F	
0.0 0.0 0.0 1.0							CARD G	
							CARD H	
							CARD I	
1.0 1.0							CARD J	
1.0 1.0							CARD K	
1.0 1.0 1.0							CARDCGA	
COMBINATORIAL GEOMETRY DATA								
SPH 1 0 0 0 30.00							CARDCGB	
SPH 2 0 0 0 35.00							CARDCGB	
SPH 3 0 0 0 1.E+03							CARDCGB	
END							CARDCGC	
ZON 1							CARDCGC	
ZON -1 2							CARDCGC	
ZON -2 3							CARDCGC	
END							CARDCGD	
1 2 3							CARDCGE	
1000 1 1000							CARD S	
1 0 0							CARD T	
1.00							CARD X	
0.0 0. 0.0 1							CARD X	
0.0 0.5 0.0 1							CARD X	
0.0 1. 0.0 1							CARD X	
0.0 3. 0.0 1							CARD X	
0.0 5. 0.0 1							CARD X	
0.0 7. 0.0 1							CARD X	
0.0 10. 0.0 1							CARD X	
0.0 15. 0.0 1							CARD X	
0.0 20. 0.0 1							CARD X	
0.0 25. 0.0 1							CARD X	
0.0 30. 0.0 1							CARD X	
0.0 30.1 0.0 1							CARD X	
0.0 31. 0.0 1							CARD X	
0.0 32. 0.0 1							CARD X	
0.0 35. 0.0 1							CARD X	
0.0 35.1 0.0 1							CARD X	
0.0 40. 0.0 1							CARD X	
0.0 45. 0.0 1							CARD X	
0.0 50. 0.0 1							CARD X	
0.0 60. 0.0 1							CARD X	
0.0 80. 0.0 1							CARD X	
0.0 100. 0.0 1							CARD X	
0.0 150. 0.0 1							CARD X	
0.0 200. 0.0 1							CARD X	
0.0 300. 0.0 1							CARD X	
0.0 400. 0.0 1							CARD X	
						-1	CARD Z	

Appendix A.3 Input data of sample problem 2.

1	2	3	4	5	6	7	8
PKN-H-CG	CYLINDER	GEOM.	252CF(R=25CM,Z=50CM)	VOLUME	SRC	/PKN-H/SP02/	CARD A
10	10	4	2	0	1	2	CARD B
1.0	0.0	0.0	0.0	0.0	0.0	0.0	CARD C
0.0	2.5	5.0	7.5	10.0	12.5	15.0	CARD D
20.0	22.5	25.0					CARD D
-25.	-20.	-15.	-10.	-5.	0.	5.	CARD E
15.	20.	25.					CARD E
0.0	1.5708	3.1416	4.7124	6.2832			CARD F
0.0	0.0	170.	1.0				CARD G
			-2.				CARD H
1.0	1.0	1.0	1.0	1.0	1.0	1.0	CARD I
1.0	1.0	1.0					CARD J
1.0	1.0	1.0	1.0	1.0	1.0	1.0	CARD I
1.0	1.0	1.0					CARD J
1.0	1.0	1.0	1.0	1.0			CARD K
							CARDCGA
RCC	1	0.	0.	145.	0.	0.	CARDCGB
		25.					CARDCGB
RCC	2	0.	0.	-100.	0.	0.	CARDCGB
		500.					CARDCGB
END							CARDCGC
ZON		1					CARDCGC
ZON		-1	2				CARDCGC
END							CARDCGC
1	2						CARDCGD
1	1						CARDCGE
1	0	0					CARD S
1.00							CARD T
0.00	170.	0.0	0				CARD X
0.1	170.	0.0	0				CARD X
1.00	170.	0.0	0				CARD X
2.00	170.	0.0	0				CARD X
3.00	170.	0.0	0				CARD X
5.00	170.	0.0	0				CARD X
7.00	170.	0.0	0				CARD X
10.00	170.	0.0	0				CARD X
15.00	170.	0.0	0				CARD X
20.00	170.	0.0	0				CARD X
30.00	170.	0.0	0				CARD X
50.00	170.	0.0	0				CARD X
70.00	170.	0.0	0				CARD X
100.0	170.	0.0	0				CARD X
130.0	170.	0.0	0				CARD X
160.0	170.	0.0	0				CARD X
200.0	170.	0.0	0				CARD X
240.0	170.	0.0	0				CARD X
0.00	120.	0.0	0				CARD X
0.10	120.	0.0	0				CARD X
1.00	120.	0.0	0				CARD X
2.00	120.	0.0	0				CARD X

3.00	120.	0.0	0	CARD X
5.00	120.	0.0	0	CARD X
7.00	120.	0.0	0	CARD X
10.00	120.	0.0	0	CARD X
15.00	120.	0.0	0	CARD X
20.00	120.	0.0	0	CARD X
30.00	120.	0.0	0	CARD X
50.00	120.	0.0	0	CARD X
70.00	120.	0.0	0	CARD X
100.0	120.	0.0	0	CARD X
130.0	120.	0.0	0	CARD X
160.0	120.	0.0	0	CARD X
200.0	120.	0.0	0	CARD X
240.0	120.	0.0	0	CARD X
0.00	20.	0.0	0	CARD X
0.10	20.	0.0	0	CARD X
1.00	20.	0.0	0	CARD X
2.00	20.	0.0	0	CARD X
3.00	20.	0.0	0	CARD X
5.00	20.	0.0	0	CARD X
7.00	20.	0.0	0	CARD X
10.00	20.	0.0	0	CARD X
20.00	20.	0.0	0	CARD X
30.00	20.	0.0	0	CARD X
50.00	20.	0.0	0	CARD X
70.00	20.	0.0	0	CARD X
100.0	20.	0.0	0	CARD X
130.0	20.	0.0	0	CARD X
160.0	20.	0.0	0	CARD X
200.0	20.	0.0	0	CARD X
240.0	20.	0.0	0	CARD X

-1

Appendix A.4 Input data of sample problem 3.

1	2	3	4	5	6	7	8
PKN-H-CG	252CF(BAR)	(R=2CM,Z=15CM) * POLY		/PKN-H/SP03/	CARD A		
2 4 4 2 2 0 1 2					CARD B		
1.0 0.0 0.0 0.0 0.0 0.0 0.0 0.0					CARD C		
0.0 1.0 2.0					CARD D		
25. 29. 32.5 36. 40.0					CARD E		
0.0 1.5708 3.1416 4.7124 6.2832					CARD F		
-10.0 0.0 0.0 0.25					CARD G		
0.0 10.0 0.0 0.25					CARD G		
10.0 0.0 0.0 0.25					CARD G		
0.0 -10.0 0.0 0.25					CARD G		
			-2.		CARD H		
1.0 1.0 1.0					CARD I		
1.0 1.0 1.0 1.0 1.0					CARD J		
1.0 1.0 1.0 1.0 1.0					CARD K		
					CARDCGA		
RCC 1 0. 0. 0.0 0. 0. 57.5					CARDCGB		
					CARDCGB		
RCC 2 0. 0. -100.0 0. 0. 350.0					CARDCGB		
					CARDCGB		
					CARDCGB		
END					CARDCGC		
ZON 1					CARDCGC		
ZON -1 2					CARDCGC		
END					CARDCGC		
1 2					CARDCGD		
1 1000					CARDCGE		
1 0 0					CARD S		
1.00					CARD T		
0.00 32.5 0.0 0					CARD X		
1.00 32.5 0.0 0					CARD X		
2.00 32.5 0.0 0					CARD X		
5.00 32.5 0.0 0					CARD X		
8.00 32.5 0.0 0					CARD X		
9.00 32.5 0.0 0					CARD X		
10.0 32.5 0.0 0					CARD X		
11.0 32.5 0.0 0					CARD X		
12.0 32.5 0.0 0					CARD X		
15.0 32.5 0.0 0					CARD X		
20.0 32.5 0.0 0					CARD X		
25.0 32.5 0.0 0					CARD X		
27.0 32.5 0.0 0					CARD X		
30.0 32.5 0.0 0					CARD X		
40.0 32.5 0.0 0					CARD X		
50.0 32.5 0.0 0					CARD X		
75.0 32.5 0.0 0					CARD X		
100.0 32.5 0.0 0					CARD X		
125.0 32.5 0.0 0					CARD X		
160.0 32.5 0.0 0					CARD X		
0.00 12.5 0.0 0					CARD X		
1.00 12.5 0.0 0					CARD X		
2.00 12.5 0.0 0					CARD X		
5.00 12.5 0.0 0					CARD X		

5.00	12.5	0.0	0	CARD X
8.00	12.5	0.0	0	CARD X
9.00	12.5	0.0	0	CARD X
10.0	12.5	0.0	0	CARD X
11.0	12.5	0.0	0	CARD X
12.0	12.5	0.0	0	CARD X
15.0	12.5	0.0	0	CARD X
20.0	12.5	0.0	0	CARD X
25.0	12.5	0.0	0	CARD X
27.0	12.5	0.0	0	CARD X
30.0	12.5	0.0	0	CARD X
40.0	12.5	0.0	0	CARD X
50.0	12.5	0.0	0	CARD X
75.0	12.5	0.0	0	CARD X
100.0	12.5	0.0	0	CARD X
125.0	12.5	0.0	0	CARD X
160.0	12.5	0.0	0	CARD X
0.00	32.5	0.7854	0	CARD X
1.00	32.5	0.7854	0	CARD X
2.00	32.5	0.7854	0	CARD X
5.00	32.5	0.7854	0	CARD X
8.00	32.5	0.7854	0	CARD X
9.00	32.5	0.7854	0	CARD X
10.0	32.5	0.7854	0	CARD X
11.0	32.5	0.7854	0	CARD X
12.0	32.5	0.7854	0	CARD X
15.0	32.5	0.7854	0	CARD X
20.0	32.5	0.7854	0	CARD X
25.0	32.5	0.7854	0	CARD X
27.0	32.5	0.7854	0	CARD X
30.0	32.5	0.7854	0	CARD X
40.0	32.5	0.7854	0	CARD X
50.0	32.5	0.7854	0	CARD X
75.0	32.5	0.7854	0	CARD X
100.0	32.5	0.7854	0	CARD X
125.0	32.5	0.7854	0	CARD X
160.0	32.5	0.7854	0	CARD X
0.00	12.5	0.7854	0	CARD X
1.00	12.5	0.7854	0	CARD X
2.00	12.5	0.7854	0	CARD X
5.00	12.5	0.7854	0	CARD X
8.00	12.5	0.7854	0	CARD X
10.0	12.5	0.7854	0	CARD X
12.0	12.5	0.7854	0	CARD X
15.0	12.5	0.7854	0	CARD X
20.0	12.5	0.7854	0	CARD X
25.0	12.5	0.7854	0	CARD X
30.0	12.5	0.7854	0	CARD X
40.0	12.5	0.7854	0	CARD X
50.0	12.5	0.7854	0	CARD X
75.0	12.5	0.7854	0	CARD X
100.0	12.5	0.7854	0	CARD X
125.0	12.5	0.7854	0	CARD X
160.0	12.5	0.7854	0	CARD X

0.00	32.5	0.0	0	CARD X
0.00	32.6	0.0	0	CARD X
0.00	33.5	0.0	0	CARD X
0.00	34.5	0.0	0	CARD X
0.00	37.5	0.0	0	CARD X
0.00	42.5	0.0	0	CARD X
0.00	47.5	0.0	0	CARD X
0.00	52.5	0.0	0	CARD X
0.00	57.5	0.0	0	CARD X
0.00	62.5	0.0	0	CARD X
0.00	67.5	0.0	0	CARD X
0.00	72.5	0.0	0	CARD X
0.00	82.5	0.0	0	CARD X
0.00	107.5	0.0	0	CARD X
0.00	132.5	0.0	0	CARD X
0.00	157.5	0.0	0	CARD X
0.00	192.5	0.0	0	CARD X
0.00	202.5	0.0	0	CARD X
			-1	CARD Z

Appendix A.5 Input data of sample problem 4.

	1	2	3	4	5	6	7	8
PKN-H-CG	SAMPLE	PROBLEM.04	252CF	FACILITY(11M*11M*7M)	/PKN-H-SP04/	CARD A		
2	6	4	4	0	1	2	CARD B	
1.0	0.0	0.0	0.0	0.0	0.0	0.0	CARD C	
0.0	1.0	2.0					CARD D	
-7.5	-5.0	-2.5	0.0	2.5	5.0	7.5	CARD E	
0.0	1.5708	3.1416	4.7124	6.2832			CARD F	
0.0	0.0	32.5	1.0				CARD G	
			-2.				CARD H	
1.0	1.0	1.0					CARD I	
1.0	1.0	1.0	1.0	1.0	1.0	1.0	CARD J	
1.0	1.0	1.0	1.0	1.0			CARD K	
							CARDCGA	
RCC	1	0.	0.	0.	0.	0.	57.5	CARDCGB
		25.0						CARDCGB
RPP	2	-475.	25.	-25.	475.	0.	300.	CARDCGB
RPP	3	-535.	105.	-125.	595.	-40.	340.	CARDCGB
RPP	4	-800.	300.	-300.	800.	-200.	600.	CARDCGB
END								CARDCGB
ZON		1						CARDCGC
ZON		-1	2					CARDCGC
ZON		-2	3					CARDCGC
ZON		-3	4					CARDCGC
END								CARDCGC
1	2	3	4					CARDCGD
1	1000	2	1000					CARDCGE
1	0	0						CARD S
1.00								CARD T
0.0	-160.0	0.0		1				CARD X
0.0	-120.0	0.0		1				CARD X
0.0	-90.0	0.0		1				CARD X
0.0	-60.0	0.0		1				CARD X
0.0	-40.1	0.0		1				CARD X
0.0	-39.9	0.0		1				CARD X
0.0	-20.0	0.0		1				CARD X
0.0	-10.0	0.0		1				CARD X
0.0	-0.1	0.0		1				CARD X
0.0	0.1	0.0		1				CARD X
0.0	10.0	0.0		1				CARD X
0.0	20.0	0.0		1				CARD X
0.0	25.0	0.0		1				CARD X
0.0	30.5	0.0		1				CARD X
0.0	32.5	0.0		1				CARD X
0.0	34.5	0.0		1				CARD X
0.0	40.0	0.0		1				CARD X
0.0	45.0	0.0		1				CARD X
0.0	57.4	0.0		1				CARD X
0.0	57.6	0.0		1				CARD X
0.0	70.0	0.0		1				CARD X
0.0	90.0	0.0		1				CARD X
0.0	120.0	0.0		1				CARD X
0.0	160.0	0.0		1				CARD X
0.0	220.0	0.0		1				CARD X

0.0	260.0	0.0	1	CARD X
0.0	300.0	0.0	1	CARD X
0.0	300.1	0.0	1	CARD X
0.0	310.0	0.0	1	CARD X
0.0	320.0	0.0	1	CARD X
0.0	340.0	0.0	1	CARD X
0.0	340.1	0.0	1	CARD X
0.0	380.0	0.0	1	CARD X
0.0	420.0	0.0	1	CARD X
0.0	500.0	0.0	1	CARD X
0.0	32.5	-255.0	1	CARD X
0.0	32.5	-195.0	1	CARD X
0.0	32.5	-135.0	1	CARD X
0.0	32.5	-125.0	1	CARD X
0.0	32.5	-100.0	1	CARD X
0.0	32.5	-75.0	1	CARD X
0.0	32.5	-50.0	1	CARD X
0.0	32.5	-30.0	1	CARD X
0.0	32.5	-25.0	1	CARD X
0.0	32.5	-20.0	1	CARD X
0.0	32.5	-15.0	1	CARD X
0.0	32.5	-10.0	1	CARD X
0.0	32.5	-5.0	1	CARD X
0.0	32.5	-2.0	1	CARD X
0.0	32.5	0.0	1	CARD X
0.0	32.5	2.0	1	CARD X
0.0	32.5	5.0	1	CARD X
0.0	32.5	10.0	1	CARD X
0.0	32.5	15.0	1	CARD X
0.0	32.5	20.0	1	CARD X
0.0	32.5	25.0	1	CARD X
0.0	32.5	35.0	1	CARD X
0.0	32.5	65.0	1	CARD X
0.0	32.5	105.0	1	CARD X
0.0	32.5	155.0	1	CARD X
0.0	32.5	215.0	1	CARD X
0.0	32.5	275.0	1	CARD X
0.0	32.5	355.0	1	CARD X
0.0	32.5	375.0	1	CARD X
0.0	32.5	425.0	1	CARD X
0.0	32.5	474.9	1	CARD X
0.0	32.5	475.1	1	CARD X
0.0	32.5	480.0	1	CARD X
0.0	32.5	490.0	1	CARD X
0.0	32.5	500.0	1	CARD X
0.0	32.5	515.0	1	CARD X
0.0	32.5	535.0	1	CARD X
0.0	32.5	555.0	1	CARD X
0.0	32.5	575.0	1	CARD X
0.0	32.5	594.9	1	CARD X
0.0	32.5	595.1	1	CARD X
0.0	32.5	610.0	1	CARD X
0.0	32.5	650.0	1	CARD X
0.0	32.5	750.0	1	CARD X
			-1	CARD Z

Appendix A.6 Input data of sample problem 5.

	1	2	3	4	5	6	7	8
PKN-H-CG	CYLINDER	GEOM.	250MEV(POINT)SRC *AIR*CONCRETE*AIR /PKN-H/SP05/				CARD A	
2	2	2	3	3	0	1	2	CARD B
1.0	0.0	0.0		0.0	0.0	0.0	0.0	CARD C
0.0	0.5	1.0						CARD D
-0.5	0.0	0.5						CARD E
0.0	3.1416	6.2832						CARD F
0.0	0.0	0.0		1.0				CARD G
				-2.				CARD H
1.0	1.0	1.0						CARD I
1.0	1.0	1.0						CARD J
1.0	1.0	1.0						CARD K
			GEOMETRY DATA					CARDCGA
RCC	1	0.	0.	-2000.	0.	0.	4000.	CARDCGB
		100.						CARDCGB
RCC	2	0.	0.	-2000.	0.	0.	4000.	CARDCGB
		1000.						CARDCGB
RCC	3	0.	0.	-2000.	0.	0.	4000.	CARDCGB
		4000.						CARDCGB
END								CARDCGB
ZON		1						CARDCGC
ZON		-1	2					CARDCGC
ZON		-2	3					CARDCGC
END								CARDCGC
1	2	3						CARDCGD
1000	2	1000						CARDCGE
1	7	7						CARD S
1.00								CARD T
0.00	0.	0.		0				CARD X
0.1	0.	0.		0				CARD X
5.	0.	0.		0				CARD X
10.	0.	0.		0				CARD X
20.	0.	0.		0				CARD X
30.	0.	0.		0				CARD X
50.	0.	0.		0				CARD X
80.	0.	0.		0				CARD X
90.	0.	0.		0				CARD X
100.	0.	0.		0				CARD X
110.	0.	0.		0				CARD X
120.	0.	0.		0				CARD X
150.	0.	0.		0				CARD X
200.	0.	0.		0				CARD X
250.	0.	0.		0				CARD X
300.	0.	0.		0				CARD X
350.	0.	0.		0				CARD X
400.	0.	0.		0				CARD X
500.	0.	0.		0				CARD X
600.	0.	0.		0				CARD X
700.	0.	0.		0				CARD X
800.	0.	0.		0				CARD X
900.	0.	0.		0				CARD X

1000.	0.	0.	0	CARD X
1000.1	0.	0.	0	CARD X
1100.	0.	0.	0	CARD X
1200.	0.	0.	0	CARD X
1500.	0.	0.	0	CARD X
1500.	0.	0.	0	CARD X
2000.	0.	0.	0	CARD X
2500.	0.	0.	0	CARD X
3000.	0.	0.	0	CARD X
			-1	CARD Z

Appendix A.7 Output.

Calculational results is outputted corresponding to detector points desclibing in CARD-X. Neutron and secondary gamma-ray dose equivalents calculated are listed, where the values of "finite thickness" represent the corrected one with infinite medium effect.

Appendix A.8 Output data of sample problem 1.

Attenuation of Dose Equivalent with PKN-H
 SOURCE ENERGY SE(0 - 0)=(4.000E+02 - 4.140E-07)(MEV) SRC POINTS = 2
 < ²⁵²Cf FISSION NEUTRON SOURCE >

Num	X ₁ (R,x,R)	X ₂ (Z,z, θ)	X ₃ (θ ,y, ϕ)	Dose Equivalent			
				infinite thickness neutron [(Sv/hr)/(n/sec)]	2nd. γ 0.000E+00	infinite thickness neutron [(Sv/hr)/(n/sec)]	2nd. γ 0.000E+00
1	0.00	0.00	0.00	3.895E-07	0.000E+00	3.895E-07	0.000E+00
2	0.00	0.50	0.00	1.947E-07	0.000E+00	1.947E-07	0.000E+00
3	0.00	1.00	0.00	7.790E-08	0.000E+00	7.790E-08	0.000E+00
4	0.00	3.00	0.00	1.053E-08	0.000E+00	1.053E-08	0.000E+00
5	0.00	5.00	0.00	3.856E-09	0.000E+00	3.856E-09	0.000E+00
6	0.00	7.00	0.00	1.977E-09	0.000E+00	1.977E-09	0.000E+00
7	0.00	10.00	0.00	9.713E-10	0.000E+00	9.713E-10	0.000E+00
8	0.00	15.00	0.00	4.323E-10	0.000E+00	4.323E-10	0.000E+00
9	0.00	20.00	0.00	2.433E-10	0.000E+00	2.433E-10	0.000E+00
10	0.00	25.00	0.00	1.557E-10	0.000E+00	1.557E-10	0.000E+00
11	0.00	30.00	0.00	1.082E-10	0.000E+00	1.082E-10	0.000E+00
12	0.00	30.10	0.00	2.417E-10	2.487E-12	2.417E-10	2.487E-12
13	0.00	31.00	0.00	2.028E-10	2.349E-12	2.028E-10	2.349E-12
14	0.00	32.00	0.00	1.672E-10	2.208E-12	1.672E-10	2.208E-12
15	0.00	35.00	0.00	9.512E-11	1.846E-12	9.512E-11	1.846E-12
16	0.00	35.10	0.00	9.458E-11	1.836E-12	7.093E-11	2.570E-13
17	0.00	40.00	0.00	7.283E-11	1.414E-12	5.462E-11	1.979E-13
18	0.00	45.00	0.00	5.754E-11	1.117E-12	4.316E-11	1.564E-13
19	0.00	50.00	0.00	4.661E-11	9.048E-13	3.496E-11	1.267E-13
20	0.00	60.00	0.00	3.237E-11	6.283E-13	2.428E-11	8.797E-14
21	0.00	80.00	0.00	1.821E-11	3.534E-13	1.366E-11	4.948E-14
22	0.00	100.00	0.00	1.165E-11	2.262E-13	8.740E-12	3.167E-14
23	0.00	150.00	0.00	5.180E-12	1.005E-13	3.885E-12	1.408E-14
24	0.00	200.00	0.00	2.914E-12	5.655E-14	2.185E-12	7.917E-15
25	0.00	300.00	0.00	1.295E-12	2.513E-14	9.712E-13	3.519E-15
26	0.00	400.00	0.00	7.284E-13	1.414E-14	5.463E-13	1.979E-15

Appendix A.9 Output data of sample problem 2.

ATTENUATION OF DOSE EQUIVALENT WITH PKN-H
 SOURCE ENERGY SE(0 - 0) = (4.000E+02 - 4.140E-07)(MEV) SRC POINTS = 400
 < ²⁵²Cf FISSION NEUTRON SOURCE >

Num	X ₁ (R,x,R)	X ₂ (Z,z, θ)	X ₃ (θ ,y, ϕ)	Dose Equivalent			
				infinite thickness neutron [(Sv/hr)/(n/sec)]	2nd. γ	finite thickness neutron [(Sv/hr)/(n/sec)]	2nd. γ
1	0.00	170.00	0.00	1.773E-10	7.321E-12	1.773E-10	7.321E-12
2	0.10	170.00	0.00	1.773E-10	7.320E-12	1.773E-10	7.320E-12
3	1.00	170.00	0.00	1.760E-10	7.301E-12	1.760E-10	7.301E-12
4	2.00	170.00	0.00	1.714E-10	7.234E-12	1.714E-10	7.234E-12
5	3.00	170.00	0.00	1.641E-10	7.123E-12	1.641E-10	7.123E-12
6	5.00	170.00	0.00	1.437E-10	6.787E-12	1.437E-10	6.787E-12
7	7.00	170.00	0.00	1.218E-10	6.371E-12	1.218E-10	6.371E-12
8	10.00	170.00	0.00	9.282E-11	5.694E-12	9.282E-11	5.694E-12
9	15.00	170.00	0.00	5.603E-11	4.522E-12	5.603E-11	4.522E-12
10	20.00	170.00	0.00	3.130E-11	3.421E-12	3.130E-11	3.421E-12
11	30.00	170.00	0.00	7.942E-12	1.802E-12	7.942E-12	1.802E-12
12	50.00	170.00	0.00	4.116E-13	4.980E-13	4.116E-13	4.980E-13
13	70.00	170.00	0.00	2.525E-14	1.497E-13	2.525E-14	1.497E-13
14	100.00	170.00	0.00	5.641E-16	2.617E-14	5.641E-16	2.617E-14
15	130.00	170.00	0.00	1.796E-17	4.724E-15	1.796E-17	4.724E-15
16	160.00	170.00	0.00	7.442E-19	8.984E-16	7.442E-19	8.984E-16
17	200.00	170.00	0.00	1.474E-20	1.124E-16	1.474E-20	1.124E-16
18	240.00	170.00	0.00	4.063E-22	1.691E-17	4.063E-22	1.691E-17
19	0.00	120.00	0.00	8.044E-13	5.847E-13	8.044E-13	5.847E-13
20	0.10	120.00	0.00	8.044E-13	5.847E-13	8.044E-13	5.847E-13
21	1.00	120.00	0.00	8.037E-13	5.844E-13	8.037E-13	5.844E-13
22	2.00	120.00	0.00	8.015E-13	5.834E-13	8.015E-13	5.834E-13
23	3.00	120.00	0.00	7.978E-13	5.817E-13	7.978E-13	5.817E-13
24	5.00	120.00	0.00	7.860E-13	5.763E-13	7.860E-13	5.763E-13
25	7.00	120.00	0.00	7.678E-13	5.684E-13	7.678E-13	5.684E-13
26	10.00	120.00	0.00	7.284E-13	5.517E-13	7.284E-13	5.517E-13
27	15.00	120.00	0.00	6.318E-13	5.124E-13	6.318E-13	5.124E-13
28	20.00	120.00	0.00	5.077E-13	4.619E-13	5.077E-13	4.619E-13
29	30.00	120.00	0.00	2.622E-13	3.467E-13	2.622E-13	3.467E-13
30	50.00	120.00	0.00	3.891E-14	1.579E-13	3.891E-14	1.579E-13
31	70.00	120.00	0.00	4.391E-15	6.231E-14	4.391E-15	6.231E-14
32	100.00	120.00	0.00	1.654E-16	1.372E-14	1.654E-16	1.372E-14
33	130.00	120.00	0.00	7.148E-18	2.860E-15	7.148E-18	2.860E-15
34	160.00	120.00	0.00	3.611E-19	6.033E-16	3.611E-19	6.033E-16
35	200.00	120.00	0.00	8.533E-21	8.350E-17	8.533E-21	8.350E-17
36	240.00	120.00	0.00	2.662E-22	1.346E-17	2.662E-22	1.346E-17
37	0.00	20.00	0.00	2.763E-18	1.691E-15	2.763E-18	1.691E-15
38	0.10	20.00	0.00	2.763E-18	1.691E-15	2.763E-18	1.691E-15
39	1.00	20.00	0.00	2.763E-18	1.691E-15	2.763E-18	1.691E-15
40	2.00	20.00	0.00	2.760E-18	1.690E-15	2.760E-18	1.690E-15
41	3.00	20.00	0.00	2.755E-18	1.689E-15	2.755E-18	1.689E-15
42	5.00	20.00	0.00	2.740E-18	1.684E-15	2.740E-18	1.684E-15
43	7.00	20.00	0.00	2.717E-18	1.676E-15	2.717E-18	1.676E-15
44	10.00	20.00	0.00	2.670E-18	1.660E-15	2.670E-18	1.660E-15
45	20.00	20.00	0.00	2.408E-18	1.571E-15	2.408E-18	1.571E-15
46	30.00	20.00	0.00	2.031E-18	1.434E-15	2.031E-18	1.434E-15
47	50.00	20.00	0.00	1.191E-18	1.080E-15	1.191E-18	1.080E-15

JAERI-Data/Code 95-004

48	70.00	20.00	0.00	5.539E-19	7.199E-16	5.539E-19	7.199E-16
49	100.00	20.00	0.00	1.239E-19	3.267E-16	1.239E-19	3.267E-16
50	130.00	20.00	0.00	2.068E-20	1.275E-16	2.068E-20	1.275E-16
51	160.00	20.00	0.00	2.917E-21	4.577E-17	2.917E-21	4.577E-17
52	200.00	20.00	0.00	1.943E-22	1.110E-17	1.943E-22	1.110E-17
53	240.00	20.00	0.00	1.363E-23	2.635E-18	1.363E-23	2.635E-18

Appendix A.10 Output data of sample problem 3.

ATTENUATION OF DOSE EQUIVALENT WITH PKN-H
 SOURCE ENERGY SE(0 - 0)=(4.000E+02 - 4.140E-07)(MEV) SOURCE POINTS = 32
 < ²⁵²Cf FISSION NEUTRON SOURCE >

Num	X ₁ (R,x,R)	X ₂ (Z,z, θ)	X ₃ (θ ,y, ϕ)	Dose Equivalent			
				infinite thickness neutron [(Sv/hr)/(n/sec)]	2nd. γ	finite thickness neutron [(Sv/hr)/(n/sec)]	2nd. γ
1	0.00	32.50	0.00	5.019E-10	1.940E-11	5.019E-10	1.940E-11
2	1.00	32.50	0.00	5.113E-10	1.954E-11	5.113E-10	1.954E-11
3	2.00	32.50	0.00	5.422E-10	2.000E-11	5.422E-10	2.000E-11
4	5.00	32.50	0.00	9.184E-10	2.537E-11	9.184E-10	2.537E-11
5	8.00	32.50	0.00	3.048E-09	5.233E-11	3.048E-09	5.233E-11
6	9.00	32.50	0.00	4.293E-09	6.718E-11	4.293E-09	6.718E-11
7	10.00	32.50	0.00	4.795E-09	7.288E-11	4.795E-09	7.288E-11
8	11.00	32.50	0.00	4.260E-09	6.592E-11	4.260E-09	6.592E-11
9	12.00	32.50	0.00	2.980E-09	4.981E-11	2.980E-09	4.981E-11
10	15.00	32.50	0.00	7.427E-10	1.906E-11	7.427E-10	1.906E-11
11	20.00	32.50	0.00	1.396E-10	7.288E-12	1.396E-10	7.288E-12
12	25.00	32.50	0.00	3.861E-11	3.852E-12	3.807E-11	3.795E-12
13	27.00	32.50	0.00	3.152E-11	3.195E-12	2.287E-11	2.137E-12
14	30.00	32.50	0.00	2.407E-11	2.495E-12	1.748E-11	1.676E-12
15	40.00	32.50	0.00	1.203E-11	1.319E-12	8.749E-12	8.947E-13
16	50.00	32.50	0.00	7.255E-12	8.217E-13	5.279E-12	5.606E-13
17	75.00	32.50	0.00	3.019E-12	3.561E-13	2.199E-12	2.445E-13
18	100.00	32.50	0.00	1.653E-12	1.986E-13	1.204E-12	1.367E-13
19	125.00	32.50	0.00	1.042E-12	1.265E-13	7.597E-13	8.723E-14
20	160.00	32.50	0.00	6.288E-13	7.699E-14	4.583E-13	5.314E-14
21	0.00	12.50	0.00	3.660E-11	4.390E-12	3.660E-11	4.390E-12
22	1.00	12.50	0.00	3.656E-11	4.385E-12	3.656E-11	4.385E-12
23	2.00	12.50	0.00	3.643E-11	4.368E-12	3.643E-11	4.368E-12
24	5.00	12.50	0.00	3.544E-11	4.249E-12	3.544E-11	4.249E-12
25	8.00	12.50	0.00	3.324E-11	4.026E-12	3.324E-11	4.026E-12
26	9.00	12.50	0.00	3.215E-11	3.929E-12	3.215E-11	3.929E-12
27	10.00	12.50	0.00	3.087E-11	3.821E-12	3.087E-11	3.821E-12
28	11.00	12.50	0.00	2.940E-11	3.703E-12	2.940E-11	3.703E-12
29	12.00	12.50	0.00	2.776E-11	3.576E-12	2.776E-11	3.576E-12
30	15.00	12.50	0.00	2.217E-11	3.158E-12	2.217E-11	3.158E-12
31	20.00	12.50	0.00	1.307E-11	2.436E-12	1.307E-11	2.436E-12
32	25.00	12.50	0.00	6.827E-12	1.813E-12	6.418E-12	1.746E-12
33	27.00	12.50	0.00	7.227E-12	1.676E-12	5.336E-12	1.288E-12
34	30.00	12.50	0.00	7.411E-12	1.481E-12	5.453E-12	1.118E-12
35	40.00	12.50	0.00	6.353E-12	9.844E-13	4.646E-12	7.169E-13
36	50.00	12.50	0.00	4.876E-12	6.820E-13	3.558E-12	4.872E-13
37	75.00	12.50	0.00	2.550E-12	3.279E-13	1.858E-12	2.298E-13
38	100.00	12.50	0.00	1.506E-12	1.896E-13	1.098E-12	1.319E-13
39	125.00	12.50	0.00	9.831E-13	1.228E-13	7.166E-13	8.526E-14
40	160.00	12.50	0.00	6.070E-13	7.561E-14	4.424E-13	5.240E-14
41	0.00	32.50	0.79	5.019E-10	1.940E-11	5.019E-10	1.940E-11
42	1.00	32.50	0.79	5.109E-10	1.954E-11	5.109E-10	1.954E-11
43	2.00	32.50	0.79	5.368E-10	1.992E-11	5.368E-10	1.992E-11
44	5.00	32.50	0.79	6.660E-10	2.168E-11	6.660E-10	2.168E-11
45	8.00	32.50	0.79	6.765E-10	2.111E-11	6.765E-10	2.111E-11
46	9.00	32.50	0.79	6.253E-10	1.994E-11	6.253E-10	1.994E-11
47	10.00	32.50	0.79	5.561E-10	1.843E-11	5.561E-10	1.843E-11

48	11.00	32.50	0.79	4.791E-10	1.674E-11	4.791E-10	1.674E-11
49	12.00	32.50	0.79	4.028E-10	1.502E-11	4.028E-10	1.502E-11
50	15.00	32.50	0.79	2.200E-10	1.048E-11	2.200E-10	1.048E-11
51	20.00	32.50	0.79	7.437E-11	5.815E-12	7.437E-11	5.815E-12
52	25.00	32.50	0.79	2.620E-11	3.468E-12	2.620E-11	3.468E-12
53	27.00	32.50	0.79	2.288E-11	2.953E-12	1.670E-11	2.039E-12
54	30.00	32.50	0.79	1.883E-11	2.368E-12	1.373E-11	1.631E-12
55	40.00	32.50	0.79	1.071E-11	1.297E-12	7.799E-12	8.916E-13
56	50.00	32.50	0.79	6.808E-12	8.161E-13	4.955E-12	5.624E-13
57	75.00	32.50	0.79	2.965E-12	3.556E-13	2.157E-12	2.464E-13
58	100.00	32.50	0.79	1.645E-12	1.984E-13	1.197E-12	1.380E-13
59	125.00	32.50	0.79	1.044E-12	1.264E-13	7.593E-13	8.821E-14
60	160.00	32.50	0.79	6.319E-13	7.693E-14	4.597E-13	5.379E-14
61	0.00	12.50	0.79	3.660E-11	4.390E-12	3.660E-11	4.390E-12
62	1.00	12.50	0.79	3.656E-11	4.385E-12	3.656E-11	4.385E-12
63	2.00	12.50	0.79	3.642E-11	4.368E-12	3.642E-11	4.368E-12
64	5.00	12.50	0.79	3.525E-11	4.244E-12	3.525E-11	4.244E-12
65	8.00	12.50	0.79	3.240E-11	4.005E-12	3.240E-11	4.005E-12
66	10.00	12.50	0.79	2.944E-11	3.784E-12	2.944E-11	3.784E-12
67	12.00	12.50	0.79	2.585E-11	3.524E-12	2.585E-11	3.524E-12
68	15.00	12.50	0.79	2.001E-11	3.094E-12	2.001E-11	3.094E-12
69	20.00	12.50	0.79	1.151E-11	2.380E-12	1.151E-11	2.380E-12
70	25.00	12.50	0.79	6.020E-12	1.775E-12	6.020E-12	1.775E-12
71	30.00	12.50	0.79	6.566E-12	1.458E-12	4.851E-12	1.103E-12
72	40.00	12.50	0.79	5.859E-12	9.771E-13	4.297E-12	7.072E-13
73	50.00	12.50	0.79	4.633E-12	6.794E-13	3.387E-12	4.829E-13
74	75.00	12.50	0.79	2.508E-12	3.276E-13	1.828E-12	2.298E-13
75	100.00	12.50	0.79	1.500E-12	1.894E-13	1.092E-12	1.326E-13
76	125.00	12.50	0.79	9.844E-13	1.228E-13	7.166E-13	8.596E-14
77	160.00	12.50	0.79	6.100E-13	7.555E-14	4.439E-13	5.295E-14
78	0.00	32.50	0.00	5.019E-10	1.940E-11	5.019E-10	1.940E-11
79	0.00	32.60	0.00	5.019E-10	1.940E-11	5.019E-10	1.940E-11
80	0.00	33.50	0.00	4.986E-10	1.931E-11	4.986E-10	1.931E-11
81	0.00	34.50	0.00	4.885E-10	1.902E-11	4.885E-10	1.902E-11
82	0.00	37.50	0.00	4.200E-10	1.711E-11	4.200E-10	1.711E-11
83	0.00	42.50	0.00	2.326E-10	1.179E-11	2.326E-10	1.179E-11
84	0.00	47.50	0.00	9.570E-11	7.168E-12	9.570E-11	7.168E-12
85	0.00	52.50	0.00	3.660E-11	4.390E-12	3.660E-11	4.390E-12
86	0.00	57.50	0.00	1.428E-11	2.807E-12	1.428E-11	2.807E-12
87	0.00	62.50	0.00	1.097E-11	2.021E-12	8.090E-12	1.492E-12
88	0.00	67.50	0.00	8.512E-12	1.516E-12	6.269E-12	1.113E-12
89	0.00	72.50	0.00	6.725E-12	1.175E-12	4.951E-12	8.607E-13
90	0.00	82.50	0.00	4.443E-12	7.628E-13	3.269E-12	5.573E-13
91	0.00	107.50	0.00	2.019E-12	3.432E-13	1.485E-12	2.506E-13
92	0.00	132.50	0.00	1.139E-12	1.938E-13	8.378E-13	1.416E-13
93	0.00	157.50	0.00	7.285E-13	1.242E-13	5.359E-13	9.081E-14
94	0.00	192.50	0.00	4.438E-13	7.587E-14	3.265E-13	5.552E-14
95	0.00	202.50	0.00	3.929E-13	6.722E-14	2.890E-13	4.919E-14

Appendix A.11 Output data of sample problem 4.

ATTENUATION OF DOSE EQUIVALENT WITH PKN-H
 Source Energy SE(0 - 0)=(4.000E+02 - 4.140E-07)(MEV) SOURCE POINTS = 48
 < ^{252}Cf FISSION NEUTRON SOURCE >

Num	X_1 (R,x,R)	X_2 (Z,z, θ)	X_3 (θ ,y, ϕ)	Dose Equivalent			
				infinite thickness neutron [(Sv/hr)/(n/sec)]	2nd. γ	finite thickness neutron [(Sv/hr)/(n/sec)]	2nd. γ
1	0.00	-160.00	0.00	5.163E-15	5.920E-15	2.586E-15	5.017E-15
2	0.00	-120.00	0.00	8.281E-15	9.465E-15	4.148E-15	8.019E-15
3	0.00	-90.00	0.00	1.294E-14	1.473E-14	6.480E-15	1.248E-14
4	0.00	-60.00	0.00	2.300E-14	2.603E-14	1.152E-14	2.204E-14
5	0.00	-40.10	0.00	3.795E-14	4.264E-14	1.901E-14	3.609E-14
6	0.00	-39.90	0.00	3.849E-14	4.315E-14	3.849E-14	4.315E-14
7	0.00	-20.00	0.00	3.837E-13	2.605E-13	3.837E-13	2.605E-13
8	0.00	-10.00	0.00	1.330E-12	6.591E-13	1.330E-12	6.591E-13
9	0.00	-0.10	0.00	5.087E-12	1.740E-12	5.087E-12	1.740E-12
10	0.00	0.10	0.00	5.258E-12	1.772E-12	5.258E-12	1.772E-12
11	0.00	10.00	0.00	3.988E-11	4.498E-12	3.988E-11	4.498E-12
12	0.00	20.00	0.00	6.806E-10	2.112E-11	6.806E-10	2.112E-11
13	0.00	25.00	0.00	1.199E-08	1.688E-10	1.199E-08	1.688E-10
14	0.00	30.50	0.00	2.780E-08	3.640E-10	2.780E-08	3.640E-10
15	0.00	32.50	0.00	2.348E-08	3.185E-10	2.348E-08	3.185E-10
16	0.00	34.50	0.00	2.780E-08	3.640E-10	2.780E-08	3.640E-10
17	0.00	40.00	0.00	1.199E-08	1.688E-10	1.199E-08	1.688E-10
18	0.00	45.00	0.00	6.806E-10	2.112E-11	6.806E-10	2.112E-11
19	0.00	57.40	0.00	2.344E-11	3.491E-12	2.344E-11	3.491E-12
20	0.00	57.60	0.00	2.273E-11	3.426E-12	1.667E-11	2.439E-12
21	0.00	70.00	0.00	9.227E-12	1.453E-12	6.775E-12	1.044E-12
22	0.00	90.00	0.00	3.702E-12	6.018E-13	2.720E-12	4.356E-13
23	0.00	120.00	0.00	1.547E-12	2.568E-13	1.137E-12	1.867E-13
24	0.00	160.00	0.00	7.154E-13	1.203E-13	5.260E-13	8.769E-14
25	0.00	220.00	0.00	3.269E-13	5.545E-14	2.404E-13	4.050E-14
26	0.00	260.00	0.00	2.211E-13	3.763E-14	1.626E-13	2.751E-14
27	0.00	300.00	0.00	1.594E-13	2.720E-14	1.173E-13	1.989E-14
28	0.00	300.10	0.00	1.582E-13	2.711E-14	1.582E-13	2.711E-14
29	0.00	310.00	0.00	7.050E-14	1.830E-14	7.050E-14	1.830E-14
30	0.00	320.00	0.00	3.047E-14	1.133E-14	3.047E-14	1.133E-14
31	0.00	340.00	0.00	5.390E-15	3.564E-15	5.390E-15	3.564E-15
32	0.00	340.10	0.00	5.387E-15	3.562E-15	3.501E-15	3.206E-16
33	0.00	380.00	0.00	4.213E-15	2.788E-15	2.739E-15	2.510E-16
34	0.00	420.00	0.00	3.383E-15	2.241E-15	2.199E-15	2.017E-16
35	0.00	500.00	0.00	2.320E-15	1.538E-15	1.508E-15	1.384E-16
36	0.00	32.50	-255.00	4.135E-17	9.929E-17	2.688E-17	8.936E-18
37	0.00	32.50	-195.00	7.062E-17	1.696E-16	4.590E-17	1.527E-17
38	0.00	32.50	-135.00	1.468E-16	3.530E-16	9.544E-17	3.177E-17
39	0.00	32.50	-125.00	1.711E-16	4.114E-16	1.711E-16	4.114E-16
40	0.00	32.50	-100.00	2.259E-15	3.452E-15	2.259E-15	3.452E-15
41	0.00	32.50	-75.00	3.296E-14	3.097E-14	3.296E-14	3.097E-14
42	0.00	32.50	-50.00	5.661E-13	2.833E-13	5.661E-13	2.833E-13
43	0.00	32.50	-30.00	7.243E-12	1.808E-12	7.243E-12	1.808E-12
44	0.00	32.50	-25.00	1.492E-11	3.025E-12	1.492E-11	3.025E-12
45	0.00	32.50	-20.00	4.164E-11	4.953E-12	4.164E-11	4.953E-12
46	0.00	32.50	-15.00	1.310E-10	8.961E-12	1.310E-10	8.961E-12
47	0.00	32.50	-10.00	5.005E-10	1.935E-11	5.005E-10	1.935E-11

48	0.00	32.50	-5.00	2.836E-09	6.093E-11	2.836E-09	6.093E-11
49	0.00	32.50	-2.00	1.298E-08	1.935E-10	1.298E-08	1.935E-10
50	0.00	32.50	0.00	2.348E-08	3.185E-10	2.348E-08	3.185E-10
51	0.00	32.50	2.00	1.298E-08	1.935E-10	1.298E-08	1.935E-10
52	0.00	32.50	5.00	2.836E-09	6.093E-11	2.836E-09	6.093E-11
53	0.00	32.50	10.00	5.005E-10	1.935E-11	5.005E-10	1.935E-11
54	0.00	32.50	15.00	1.310E-10	8.961E-12	1.310E-10	8.961E-12
55	0.00	32.50	20.00	4.164E-11	4.953E-12	4.164E-11	4.953E-12
56	0.00	32.50	25.00	1.492E-11	3.025E-12	1.471E-11	2.983E-12
57	0.00	32.50	35.00	7.853E-12	1.566E-12	5.812E-12	1.162E-12
58	0.00	32.50	65.00	2.331E-12	4.591E-13	1.724E-12	3.398E-13
59	0.00	32.50	105.00	8.984E-13	1.764E-13	6.646E-13	1.305E-13
60	0.00	32.50	155.00	4.130E-13	8.103E-14	3.055E-13	5.993E-14
61	0.00	32.50	215.00	2.148E-13	4.213E-14	1.589E-13	3.116E-14
62	0.00	32.50	275.00	1.313E-13	2.576E-14	9.715E-14	1.905E-14
63	0.00	32.50	355.00	7.882E-14	1.546E-14	5.831E-14	1.143E-14
64	0.00	32.50	375.00	7.064E-14	1.385E-14	5.226E-14	1.024E-14
65	0.00	32.50	425.00	5.500E-14	1.079E-14	4.069E-14	7.976E-15
66	0.00	32.50	474.90	4.405E-14	8.638E-15	3.258E-14	6.388E-15
67	0.00	32.50	475.10	4.369E-14	8.606E-15	4.369E-14	8.606E-15
68	0.00	32.50	480.00	2.970E-14	7.235E-15	2.970E-14	7.235E-15
69	0.00	32.50	490.00	1.326E-14	4.744E-15	1.326E-14	4.744E-15
70	0.00	32.50	500.00	5.796E-15	2.875E-15	5.796E-15	2.875E-15
71	0.00	32.50	515.00	1.621E-15	1.207E-15	1.621E-15	1.207E-15
72	0.00	32.50	535.00	2.840E-16	3.266E-16	2.840E-16	3.266E-16
73	0.00	32.50	555.00	4.834E-17	8.069E-17	4.834E-17	8.069E-17
74	0.00	32.50	575.00	8.143E-18	1.955E-17	8.143E-18	1.955E-17
75	0.00	32.50	594.90	1.389E-18	4.933E-18	1.389E-18	4.933E-18
76	0.00	32.50	595.10	1.376E-18	4.898E-18	8.944E-19	4.408E-19
77	0.00	32.50	610.00	1.310E-18	4.662E-18	8.513E-19	4.196E-19
78	0.00	32.50	650.00	1.153E-18	4.106E-18	7.498E-19	3.695E-19
79	0.00	32.50	750.00	8.664E-19	3.084E-18	5.632E-19	2.776E-19

Appendix A.12 Output data of sample problem 5.

ATTENUATION OF DOSE EQUIVALENT WITH PKN-H
 SOURCE ENERGY SE(7 - 7)=(2.500E+02 - 2.500E+02)(MEV) SOURCE POINTS = 8
 < MONOENERGETIC NEUTRON SOURCE >

Num				infinite thickness		Dose Equivalent finite thickness	
	X ₁ (R,x,R)	X ₂ (Z,z, θ)	X ₃ (θ ,y, ϕ)	neutron [(Sv/hr)/(n/sec)]	2nd. γ	neutron [(Sv/hr)/(n/sec)]	2nd. γ
1	0.00	0.00	0.00	5.718E-07	0.000E+00	5.718E-07	0.000E+00
2	0.10	0.00	0.00	5.419E-07	0.000E+00	5.419E-07	0.000E+00
3	5.00	0.00	0.00	7.008E-09	0.000E+00	7.008E-09	0.000E+00
4	10.00	0.00	0.00	1.778E-09	0.000E+00	1.778E-09	0.000E+00
5	20.00	0.00	0.00	4.461E-10	0.000E+00	4.461E-10	0.000E+00
6	30.00	0.00	0.00	1.984E-10	0.000E+00	1.984E-10	0.000E+00
7	50.00	0.00	0.00	7.146E-11	0.000E+00	7.146E-11	0.000E+00
8	80.00	0.00	0.00	2.792E-11	0.000E+00	2.792E-11	0.000E+00
9	90.00	0.00	0.00	2.206E-11	0.000E+00	2.206E-11	0.000E+00
10	100.00	0.00	0.00	1.787E-11	0.000E+00	1.787E-11	0.000E+00
11	110.00	0.00	0.00	2.681E-11	1.579E-13	2.681E-11	1.579E-13
12	120.00	0.00	0.00	2.181E-11	1.573E-13	2.181E-11	1.573E-13
13	150.00	0.00	0.00	1.183E-11	1.388E-13	1.183E-11	1.388E-13
14	200.00	0.00	0.00	4.172E-12	7.842E-14	4.172E-12	7.842E-14
15	250.00	0.00	0.00	1.387E-12	3.078E-14	1.387E-12	3.078E-14
16	300.00	0.00	0.00	4.370E-13	9.467E-15	4.370E-13	9.467E-15
17	350.00	0.00	0.00	1.331E-13	2.559E-15	1.331E-13	2.559E-15
18	400.00	0.00	0.00	4.005E-14	6.687E-16	4.005E-14	6.687E-16
19	500.00	0.00	0.00	3.737E-15	5.366E-17	3.737E-15	5.366E-17
20	600.00	0.00	0.00	3.829E-16	6.338E-18	3.829E-16	6.338E-18
21	700.00	0.00	0.00	4.158E-17	9.188E-19	4.158E-17	9.188E-19
22	800.00	0.00	0.00	4.077E-18	8.662E-20	4.077E-18	8.662E-20
23	900.00	0.00	0.00	3.997E-19	8.534E-21	3.997E-19	8.534E-21
24	1000.00	0.00	0.00	3.892E-20	8.352E-22	3.892E-20	8.352E-22
25	1000.10	0.00	0.00	3.891E-20	8.350E-22	2.727E-20	2.252E-22
26	1100.00	0.00	0.00	3.216E-20	6.902E-22	2.254E-20	1.862E-22
27	1200.00	0.00	0.00	2.703E-20	5.800E-22	1.894E-20	1.564E-22
28	1500.00	0.00	0.00	1.730E-20	3.712E-22	1.212E-20	1.001E-22
29	1500.00	0.00	0.00	1.730E-20	3.712E-22	1.212E-20	1.001E-22
30	2000.00	0.00	0.00	9.730E-21	2.088E-22	6.818E-21	5.631E-23
31	2500.00	0.00	0.00	6.227E-21	1.336E-22	4.364E-21	3.604E-23
32	3000.00	0.00	0.00	4.324E-21	9.280E-23	3.030E-21	2.503E-23

Appendix A.13 Energy spectrum of ^{252}Cf fission and $^{241}\text{Am-Be}$ neutrons.

Group	Energy (MeV)			^{252}Cf (n/sec)	$^{241}\text{Am-Be}$ (n/sec)
29	22.5	-	20.0	2.739×10^{-6}	0.0
30	20.0	-	17.5	1.653×10^{-5}	0.0
31	17.5	-	14.9	1.058×10^{-4}	0.0
32	14.9	-	13.5	2.093×10^{-4}	0.0
33	13.5	-	12.2	4.888×10^{-4}	0.0
34	12.2	-	10.0	2.848×10^{-3}	1.066×10^{-2}
35	10.0	-	8.19	8.476×10^{-3}	6.796×10^{-2}
36	8.19	-	6.70	1.944×10^{-2}	1.079×10^{-1}
37	6.70	-	5.49	3.536×10^{-2}	8.260×10^{-2}
38	5.49	-	4.49	5.494×10^{-2}	1.391×10^{-1}
39	4.49	-	3.68	7.255×10^{-2}	1.599×10^{-1}
40	3.68	-	3.01	8.722×10^{-2}	1.534×10^{-1}
41	3.01	-	2.46	9.507×10^{-2}	1.250×10^{-1}
42	2.46	-	2.02	9.355×10^{-2}	6.951×10^{-2}
43	2.02	-	1.65	9.118×10^{-2}	5.776×10^{-2}
44	1.65	-	1.35	8.178×10^{-2}	2.622×10^{-2}
45	1.35	-	1.11	6.956×10^{-2}	0.0
46	1.11	-	.970	6.068×10^{-2}	0.0
47	.907	-	.743	4.933×10^{-2}	0.0
48	.743	-	.498	7.171×10^{-2}	0.0
49	.498	-	.334	4.416×10^{-2}	0.0
50	.334	-	.224	2.620×10^{-2}	0.0
51	.224	-	.150	1.519×10^{-2}	0.0
52	.150	-	.0865	1.075×10^{-2}	0.0
53	.0865	-	.0318	6.723×10^{-3}	0.0
54	.0318	-	.0150	1.331×10^{-3}	0.0
55	.0150	-	.00710	4.330×10^{-4}	0.0
56	.00710	-	.00350	1.418×10^{-4}	0.0
57	.00350	-	.00158	4.604×10^{-5}	0.0
58	.00158	-	.000454	1.867×10^{-5}	0.0
59	.000454	-	.000101	3.041×10^{-6}	0.0

Appendix A.14 Flux to dose equivalent conversion factor of neutrons.

Flux to dose equivalent conversion factors for neutrons			
Neutron energy (MeV)	Maximum** dose equiv. ($10^{-12} \text{Sv} \cdot \text{cm}^2$)	Neutron energy (MeV)	1cm depth*** dose equiv. ($10^{-12} \text{Sv} \cdot \text{cm}^2$)
700.	1050.	20	650.
400.	630.	17.	610.
200.	508.	14.	520.
100.	469.	10.	446.
60.	450.	8.	417.
20.	425.	7.	403.
		6.	383.
		5.	378.
		4.	409.
		3.	380.
		2.	352.
		1.5	362.
		1.0	340.
		0.5	258.
		0.2	126.
		0.15	69.
		0.05	35.
		0.02	14.6
		0.01	8.6
		0.001	6.2
		1.E-4	7.1
		1.E-5	9.2
		1.E-6	11.2
		1.E-7	10.4
		2.5E-8	8.0

*) ICRP Publication 51(1987), p.39.

**) ibid., p.36.

Appendix A.15 Flux to dose equivalent conversion factor of gamma rays.

Flux to dose equivalent conversion factors for gamma rays**			
Gamma ray energy (MeV)	Maximum ⁺ dose equiv. ($10^{-12} \text{Sv} \cdot \text{cm}^2$)	Gamma ray energy (MeV)	1cm depth ⁺⁺ dose equiv. ($10^{-12} \text{Sv} \cdot \text{cm}^2$)
20.	41.6	10.	25.18
10.	24.3	8.	21.26
		6.	17.38
		5.	15.43
		4.	13.32
		3.	11.05
		2.	8.475
		1.5	6.916
		1.0	5.096
		0.8	4.280
		0.6	3.380
		0.5	2.880
		0.4	2.381
		0.3	1.808
		0.2	1.181
		0.15	0.893
		0.10	0.612
		0.08	0.531
		0.06	0.503
		0.05	0.527
		0.04	0.614
		0.03	0.786
		0.02	1.010
		0.015	0.846
		0.010	0.0743

*) ICRP Publication 51(1987), p.26

**) ibid., p.22.

Appendix A.16 Input required on CGB cards for each body type.

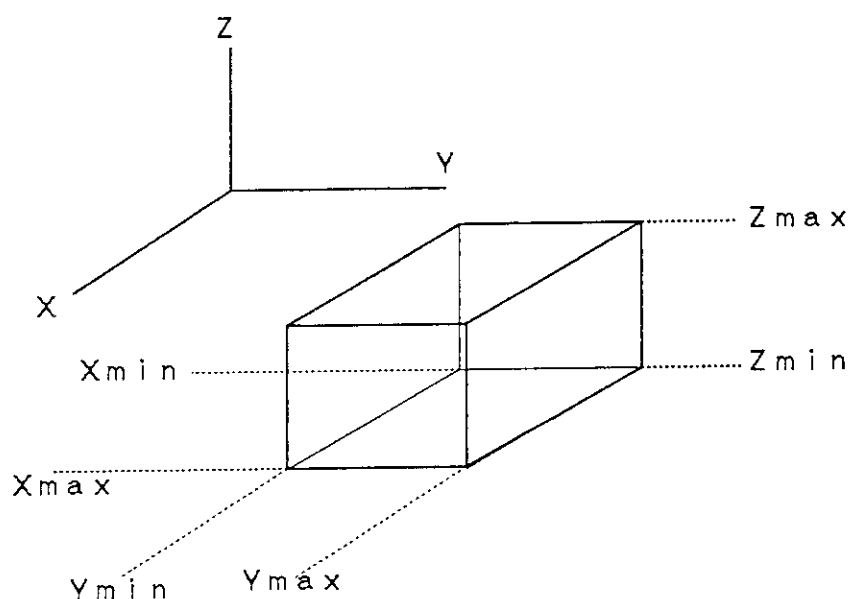
Card Columns Body Type	ITYPE A3	IALP 3-5	Real Data Defining Particular Body						Number of Cards Needed
		7-10	11-20	21-30	31-40	41-50	51-60	61-70	
Box	BOX	ILAP is assigned by the user or by the	Vx H2x Xmin Xmax Ymin Ymax Zmin Zmax	Vy H2y H3x H3y H3z	Vz H2z H3x H3y H3z	H1x H1y H1z	H1y H1z	H1z	1 of 2 2 of 2 1
Right Parall- elepiped	RPP	by the user or by the							
Sphere	SPH	code if left	Vx Vy Vz R	Vx Vy Vz R	Vy Vz R	-	-	-	1
Right Circul- ar Cylinder	RCC	blank.	Vx Vy Vz Hx Hy Hz	R - - - -	R - - - -	- - - -	- - - -	- - - -	1 of 2 2 of 2
Right Ellipt- ic Cylinder	REC		Vx Vy Vz Hx Hy Hz	R1x R1y R1z R2x R2y R2z	R1x R1y R1z R2x R2y R2z	- - - -	- - - -	- - - -	1 of 2 2 of 2
Ellipsoid	ELL		V1x V1y V1z V2x V2y V2z	V1x V1y V1z I - - -	V1x V1y V1z I - - -	V2x V2y V2z - - -	V2x V2y V2z - - -	V2x V2y V2z - - -	1 of 2 2 of 2
Truncated Right Code	TRC		Vx Vy Vz Hx Hy Hz	L1 L2 - - - -	L1 L2 - - - -	Hx Hy Hz	Hx Hy Hz	Hx Hy Hz	1 of 2 2 of 2
Right Angle Wedge	WED or RAW		Vx Vy Vz H1x H1y H1z	H2x H2y H2z H3x H3y H3z	H2x H2y H2z H3x H3y H3z	H1x H1y H1z	H1y H1z	H1z	1 of 2 2 of 2
Arbitrary Polyhedron	ARB		V1x V1y V1z V2x V2y V2z	V3x V3y V3z V4x V4y V4z	V5x V5y V5z V6x V6y V6z	V7x V7y V7z V8x V8y V8z	V7x V7y V7z V8x V8y V8z	V7x V7y V7z V8x V8y V8z	1 of 5 2 of 5 3 of 5 4 of 5 Face Descriptions (see note below) 5 of 5
Termination of Body Input Data	END								

*) from M.B. Emmett:"The MORSE Monte Carlo Radiation Transport Code System", ORNL-4972(1975), 4.3-9 to 4.3-10.

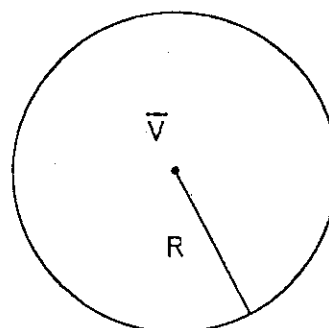
Note: Card 5 of the arbitrary polyhedron input contains a four-digit number for each of the six faces of an ARB body. The format is 6D10.3, beginning in column 11. See the ARB write-up section 4.7 in reference *) for an example.

Appendix A.17 Description of body types.

The information required to specify each type of body is as follows:

a. Rectangular Parallelepiped (RPP)

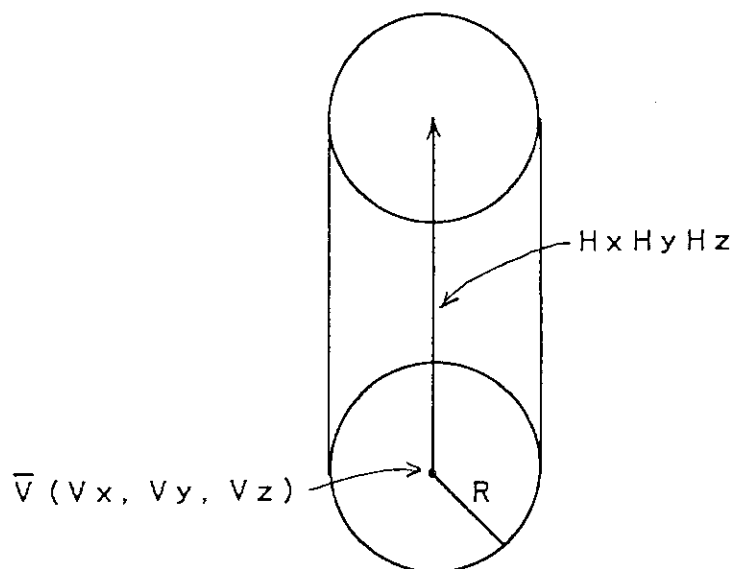
X_{\max} : the maximum value
 of x coordinates
 X_{\min} : the minimum value
 of x coordinates
 Y_{\max} : the maximum value
 of y coordinates
 Y_{\min} : the minimum value
 of y coordinates
 Z_{\max} : the maximum value
 of z coordinates
 Z_{\min} : the minimum value
 of z coordinates

b. Sphere (SPH)

R : radius
 \bar{V} : the vertex at the
 center.

*) from M.B. Emmett:"The MORSE Monte Carlo Radiation Transport Code System", ORNL-4972(1975), 4.7.3.

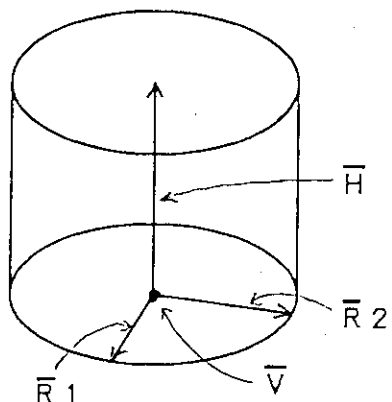
c. Right Circular Cylinder (RCC)



\bar{V} : the vertex at the center of one base.
 \bar{H} : a height vector

R : radius

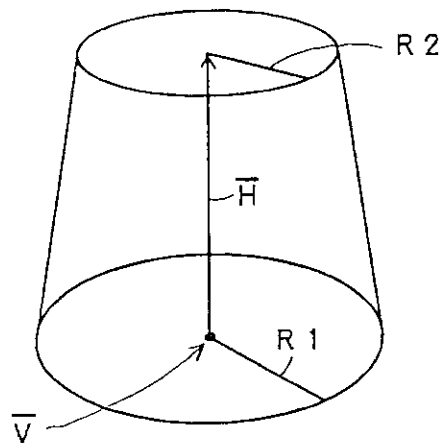
d. Right Elliptical Cylinder (REC)



\bar{V} : the vertex at the center of one base.
 \bar{H} : a height vector

\bar{R}_1, \bar{R}_2 :
 a vector in the plane of the base defining the major and minor axes.

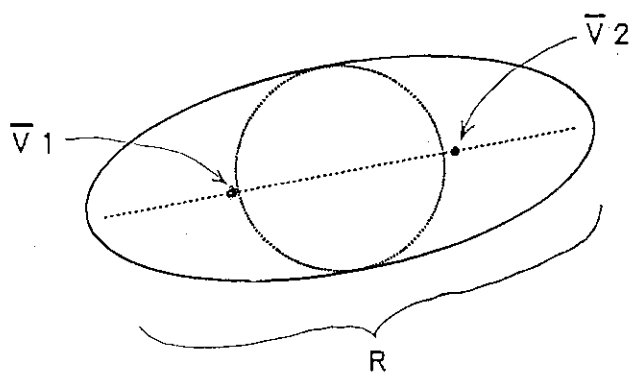
e. Truncated Right Angle Cone (TRC)



\bar{V} : the vertex at the center of one base.
 \vec{H} : a height vector

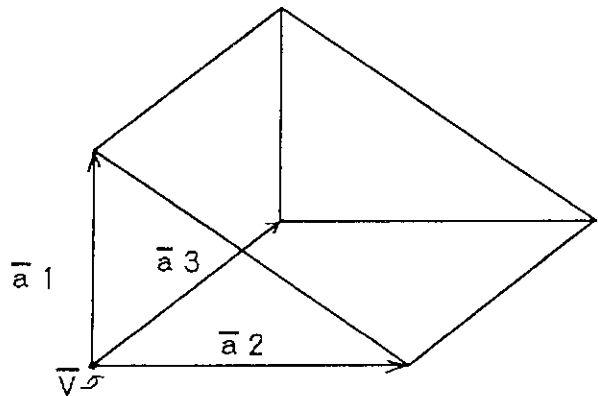
R_1, R_2 : the radii of the lower and upper bases.

f. Ellipsoid (ELL)



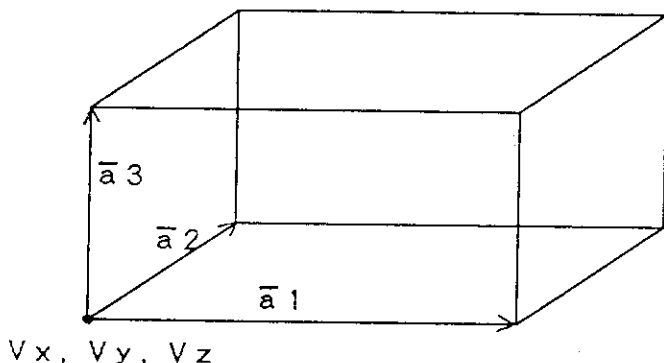
\bar{V}_1, \bar{V}_2 :
two vertices denoting the coordinates of the foci.

R : the length of the major axis.

g. Wedge (WED) or (RAW)

\bar{V} : the vertex at one of the corners.

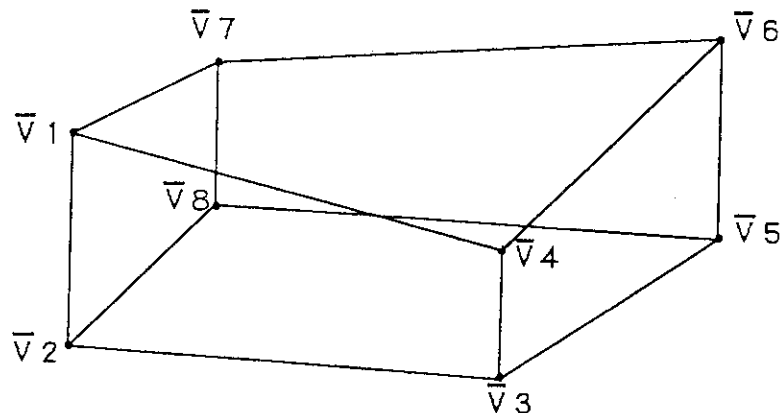
$\bar{a}_1, \bar{a}_2, \bar{a}_3$: a set of three mutually perpendicular vectors.

h. Box (BOX)

\bar{V} : the vertex at one of the corners.

$\bar{a}_1, \bar{a}_2, \bar{a}_3$: a set of three mutually perpendicular vectors.

i. Arbitrary Polyhedron (ARB)



$\bar{V}_1, \bar{V}_2, \bar{V}_3, \bar{V}_4, \bar{V}_5, \bar{V}_6, \bar{V}_7, \bar{V}_8$:
eight vertices,
must be entered in
either clockwise or
counterclockwise
order.

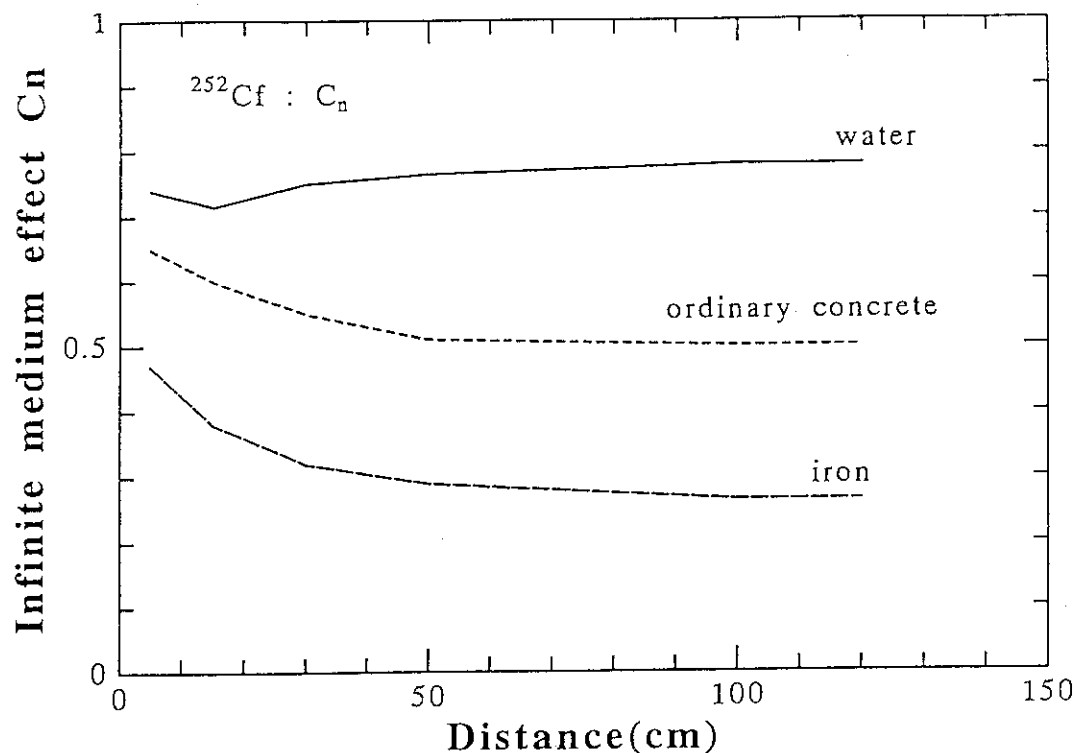
Appendix A.18 Infinite medium effect for ^{252}Cf fission and $^{241}\text{Am-Be}$ neutrons.

Fig. A.18(1) Neutron infinite medium effect coefficient C_n in water, ordinary concrete and iron at distance(cm) for ^{252}Cf fission neutrons.

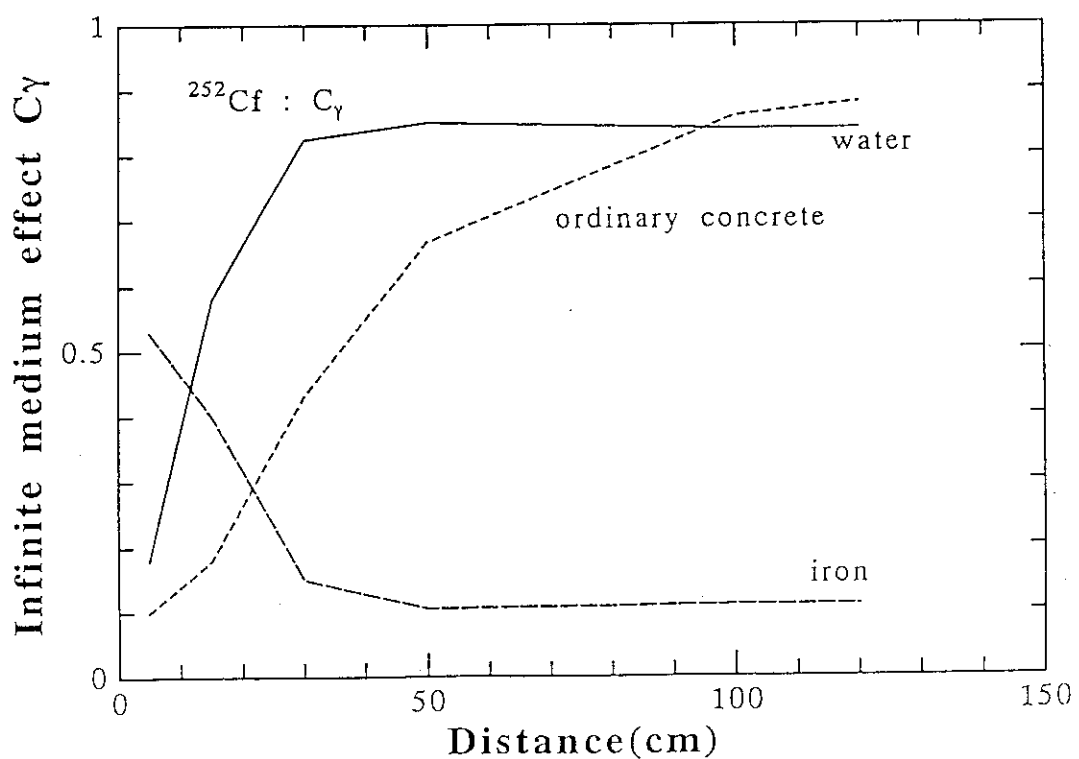


Fig. A.18(2) Secondary gamma ray infinite medium effect coefficient C_γ in water, ordinary concrete and iron at distance(cm) for ^{252}Cf fission neutrons.

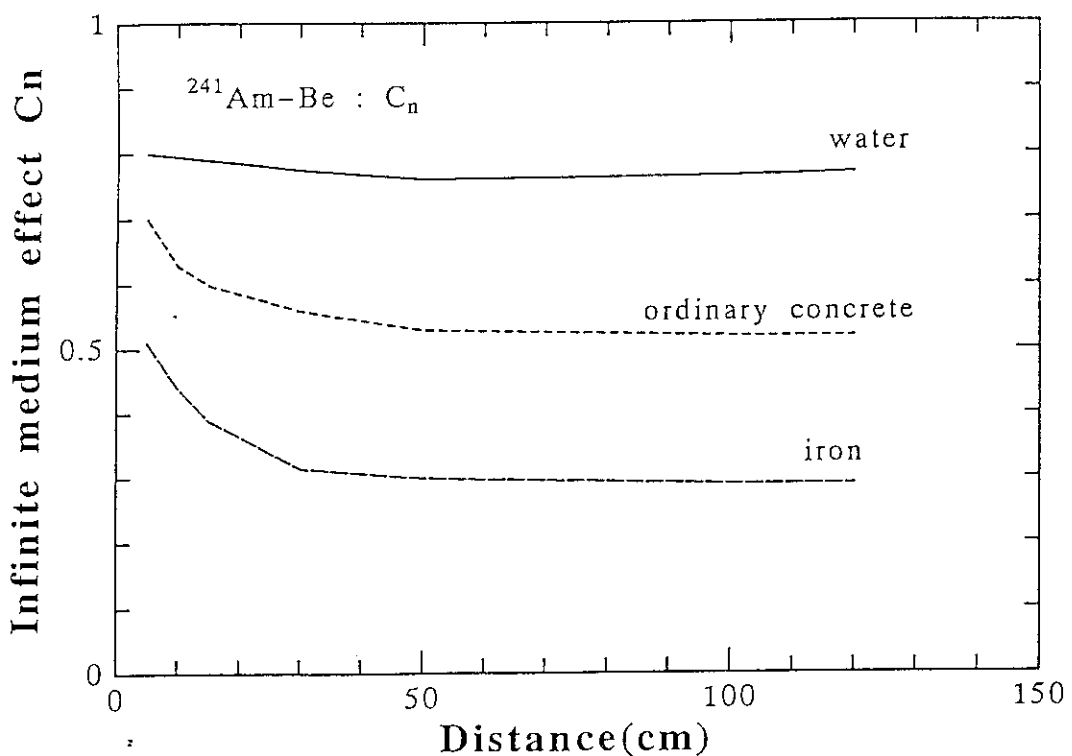


Fig. A.18(3) Neutron infinite medium effect coefficient C_n in water, ordinary concrete and iron at distance(cm) for $^{241}\text{Am-Be}$ neutrons.

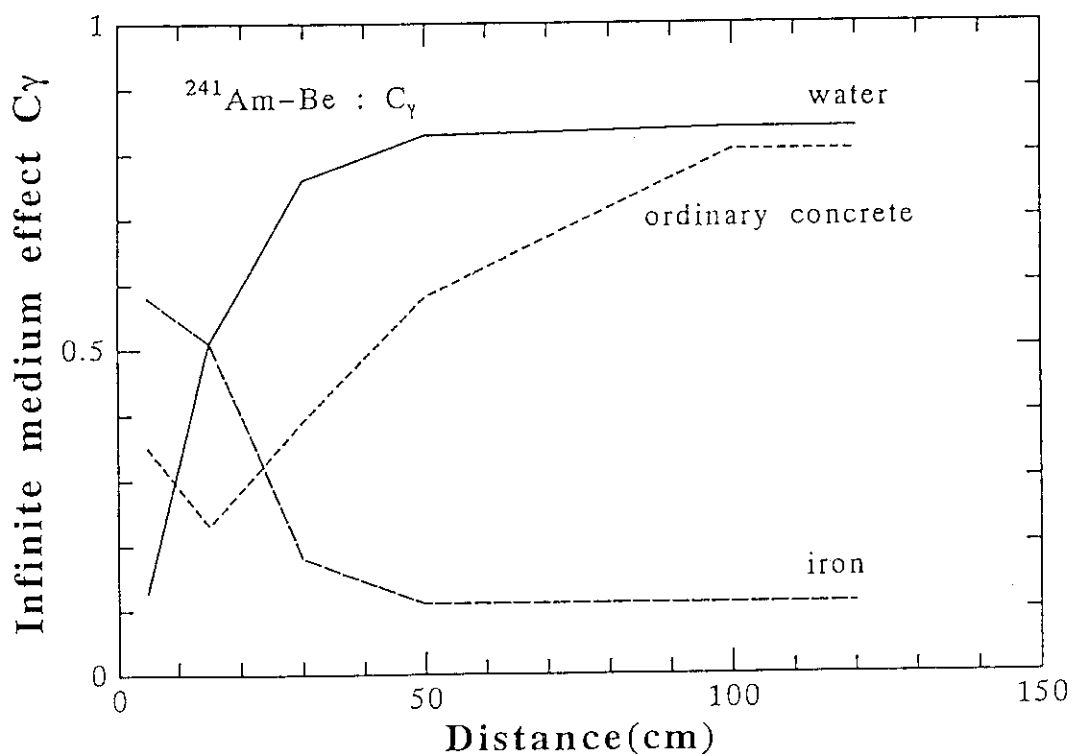


Fig. A.18(4) Secondary gamma ray infinite medium effect coefficient C_γ in water, ordinary concrete and iron at distance(cm) for $^{241}\text{Am-Be}$ neutrons.